CRANFIELD INSTITUTE OF TECHNOLOGY

SILSOE COLLEGE

M.Sc. THESIS

Academic Year 1984-85

L.L. Kiriama

The Mechanics of a disc plough

Supervisor: Professor R.J. Godwin

September 1985

This thesis is submitted in partial fulfilment of the requirements for the degree of Master of Science in Agricultural Engineering

ACKNOWLEDGEMENT

I wish to express my sincere gratitude to Professor R.J. Godwin, whose untiring guidance and encouragement throughout the period of this study is very much appreciated.

My thanks also go to Tony Reynolds and Phil Riley for their assistance in soil bin work; and to Mrs. Judith Terrell who kindly agreed to type the thesis.

I also wish to thank the British Council and the Tanzanian Government who offered me the scholarship.

Finally, I wish to thank my wife,Eli and my son, Sani for their patience and moral support.

ABSTRACT

An angle attachment was designed to enable disc axis orientation with the soil bin facility developed at the College.

A force prediction model by Godwin et al at Silsoe College was used to predict the magnitude of forces to be expected.

The effect of change in axis angle on draught, vertical and side forces was studied and the results compared with the prediction.

It was found that there was a significant effect in changing the disc axis angle. The draught and side forces were found to be less at 15^{o} than at 0^{o} axis angle. The optimum axis angle at 25^{o} sweep was found to be about 15^{o} where the maximum downward vertical force occured.

Since the experimental and predicted results did not compare well, an exploration of the force prediction model was suggested.

Whilst for global prediction the model seemed alright, it was difficult to make it work for all combinations. Although the model worked well with an 0^{o} axis angle and 90^{o} sweep angle, the edge effect and inclination for the other combinations needed greater definition.

TABLE OF CONTENTS PAGE No.

TABLE OF CONTENTS (continued) PAGE No.

TABLE OF CONTENTS (continued) PAGE No.

LIST OF TABLES, FIGURES AND PLATES

TABLE

PLATE

1.0. INTRODUCTION

With a population of over 20 million people, Tanzania depends largely on agriculture for her foreign exchange earnings. Cash crops play an important role. Cotton is one of the important crops in this category. Poor land preparation, among other factors, contributes to the decline in production year after year.

The North-western regions of Tanzania are famous for cotton production. The soils are dominated by clay loams, often known as "black cotton soils". This type of soil is very sticky when wet and extremely hard when dry. Land preparation has to be done just before the heavy rains; the time when the soils are fairly workable.

1.1. Implements used for land preparation

On small scale production, animal drawn mouldboard ploughs are used for primary cultivation. In most cases, disc ploughs are extensively used. Ridging is mostly done manually, except in large scale production where ridgers are used. In the former case, proper ploughing to a desirable depth is essential in lessening labour requirement for this operation.

1.2. The problem faced by farmers

It has always been a problem for farmers to achieve desirable ploughing depth due to hardness of soil. The plough adjustments provided by the manufacturers, in addition to timely ploughing, have not yielded satisfactory results. This prompted the author to carry out a study to find out if a helpful solution could be reached.

1.3. Proposed objectives

Two ideas were born in mind. Firstly to modify the plough by incorporating tines on the plough frame. The tines will precede and follow discs in cutting through the soil. The second idea was to change the orientation of the disc axis. This idea was opted for by the author under the supervision of Professor R.J. Godwin, who has a proficient experience in this field of study. It was hoped that the orientation of the disc axis would improve penetration without additional draft and may be a reduction in draft. However, the author intends to carry out studies on the first idea in future.

1.4. Reasons for opting for the study

Apart from finding out whether more penetration can be achieved by inclining the disc axis through various angles, the author expects to gain experience in using a soil bin. This would be quite relevant in helping to establish a facility to carry out soil bin tests at the Department of Agricultural Engineering and Land Planning of the Sokoine University of Agriculture, Morogoro, Tanzania, where the author expects to work.

1.5. Specific objectives

The design of angle attachments to enable the use of the model for prediction of forces developed by Godwin et al (8) at Silsoe College; to achieve disc axis orientation.

The analysis of the magnitude of draft, vertical and side forces will indicate whether better penetration can be achieved. Optimum axis angle can also be determined.

2.0. LITERATURE REVIEW

Standard disc ploughs usually have 2 to 6 disc blades spaced to cut 180 to 300 mm per disc. Disc tilt angles are normally 15 to 25 degrees from vertical while disc angles are 42 to 45 degrees from direction of travel, as shown in Figure 2.1. Disc diameters are commonly 610 to 710 (11).

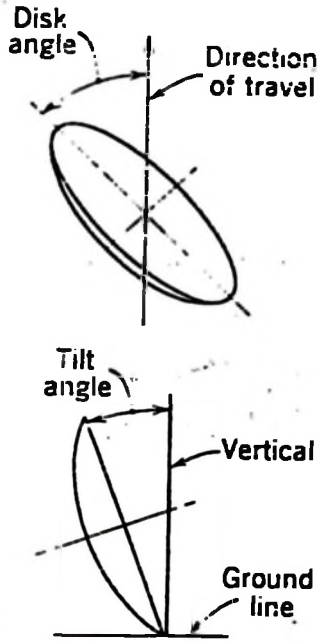

Figure 2.1. Identification of disc and tilt angle (11).

2.1. Forces acting upon a tillage tool or implement

A tillage tool moving at constant velocity is subjected to three main forces which must be in equilibrium:

(i) Force of gravity upon the implement
(ii) The passive soil forces acting upon the implement
(iii) The forces acting between the implement and the prime mover.

Clyde (2) subdivides the total soil reaction into useful and parasitic forces. He defines useful forces as those which the tool must overcome in cutting, breaking and moving the soil. Parasitic forces are those that act upon stabilizing surfaces such as the landside and sole of a plough.

Two ways of expressing the total soil reaction on a tool for the general case in which a rotation effect exists, is shown below:

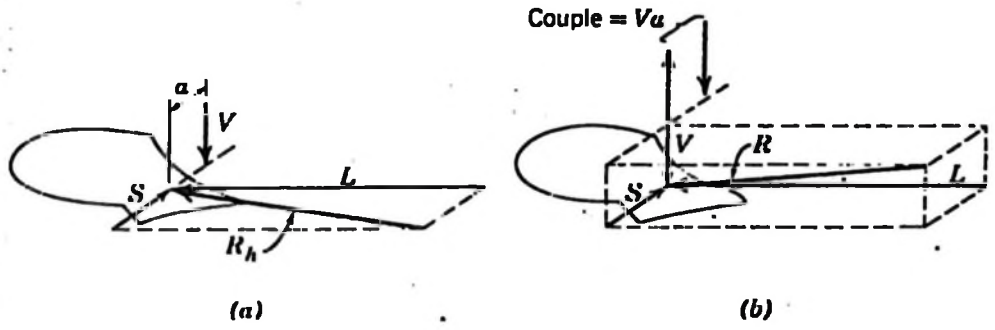

Figure 2.2. a) Two non-intersecting forces, R_h and V
b) One force, R, plus a couple, Va, in a plane perpendicular to the line of motion (2)

The force representation for a disc blade is shown in Figure 2.3. The resultant effect is expressed by two non-intersecting forces, one being a thrust force, T, parallel to the disc axis, and the other being a radial force, U.

The resultant effect is based on the longitudinal, lateral and vertical composite , L, S and V, and resultant of these forces. L and S are combined into the horizontal

resultant R_h, so that the entire effect is represented by the two non-intersecting forces, V and R_h (Figure 2.3(a)).

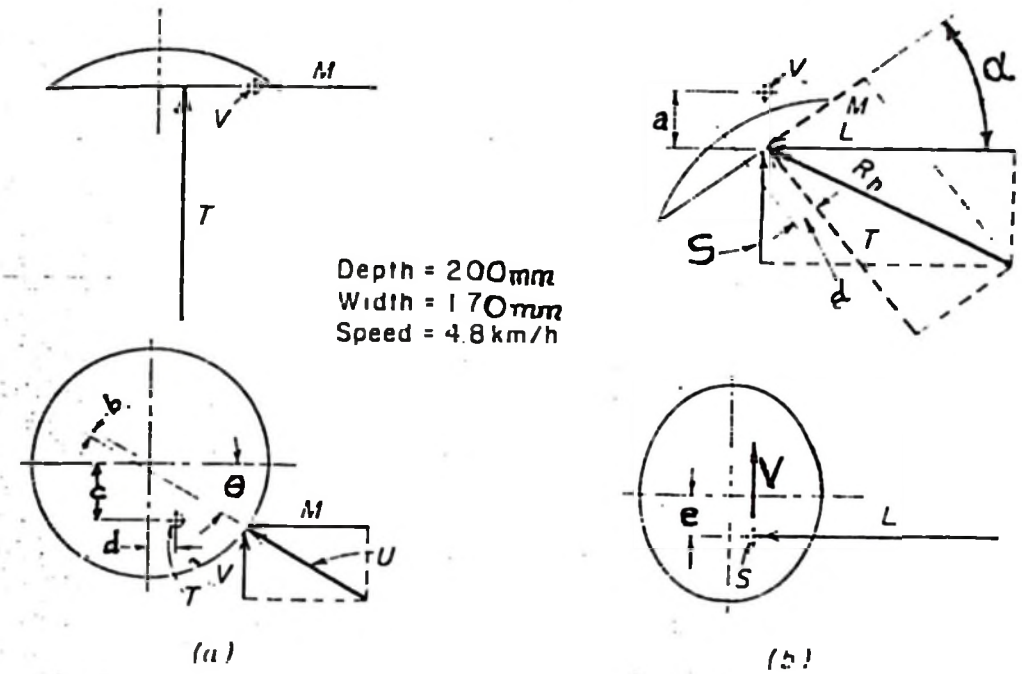

Figure 2.3 a) A thrust force T, plus a radial force U
b) A horizontal force R_h, plus a vertical force V (1)

For a 610 mm vertical disc blade under field conditions in a silt loam soil, Clyde (1) obtained the following results:

a = 159 mm, b = 16 mm, c = 156 mm, d = 64 mm
e = 117 mm, V = 0.6kN, T = 2.9kN, R_h = 2.23kN,
S = 0.98kN, θ = $31\frac{1}{4}^{o}$ and α = 38^{o}

Clyde (1) found out that the magnitude of Va couple for plough discs has usually ranged from 125 to 215 Nm, always clockwise for a right hand disc.

2.2. Factors causing variation of magnitude of forces on discs

There are several factors which affect or cause some variation in the magnitude and direction of some of the soil reaction components:

a) disc angle
b) disc velocity
c) disc geometry
d) depth of cut
e) width of cut
f) added weights
g) soil type
h) state of moisture content
i) rake angle

2.2.1. Disc angle

Harrison (10) found out that the draught and side forces increased from minimum values at 15 degrees to maximum values when the angles were between 30 to 40 degrees for draught and between 20 to 30 degrees for the side force. The vertical reaction starting from maximum values at lower angles decreased to lower values at higher angles. The increased draught at greater angles is probably due in part to the greater throw of the soil. At smaller disc angles the draught tends to increase because of greater contact area between the furrow wall and the convex (rear) side of the disc. This increasing contact is also indicated by reduction in measured side force at smaller angles, particularly in the fine sandy loam (9). Gordon (9) found out that penetration is improved by increasing the disc angle, since the upward V decreased considerably. It was also found that increasing the tilt angle with 15 to 25 degrees range normally encountered in disc ploughs, increases draught and the vertical upward force, but decreases the measured side force. Figure 2.4 (c)).

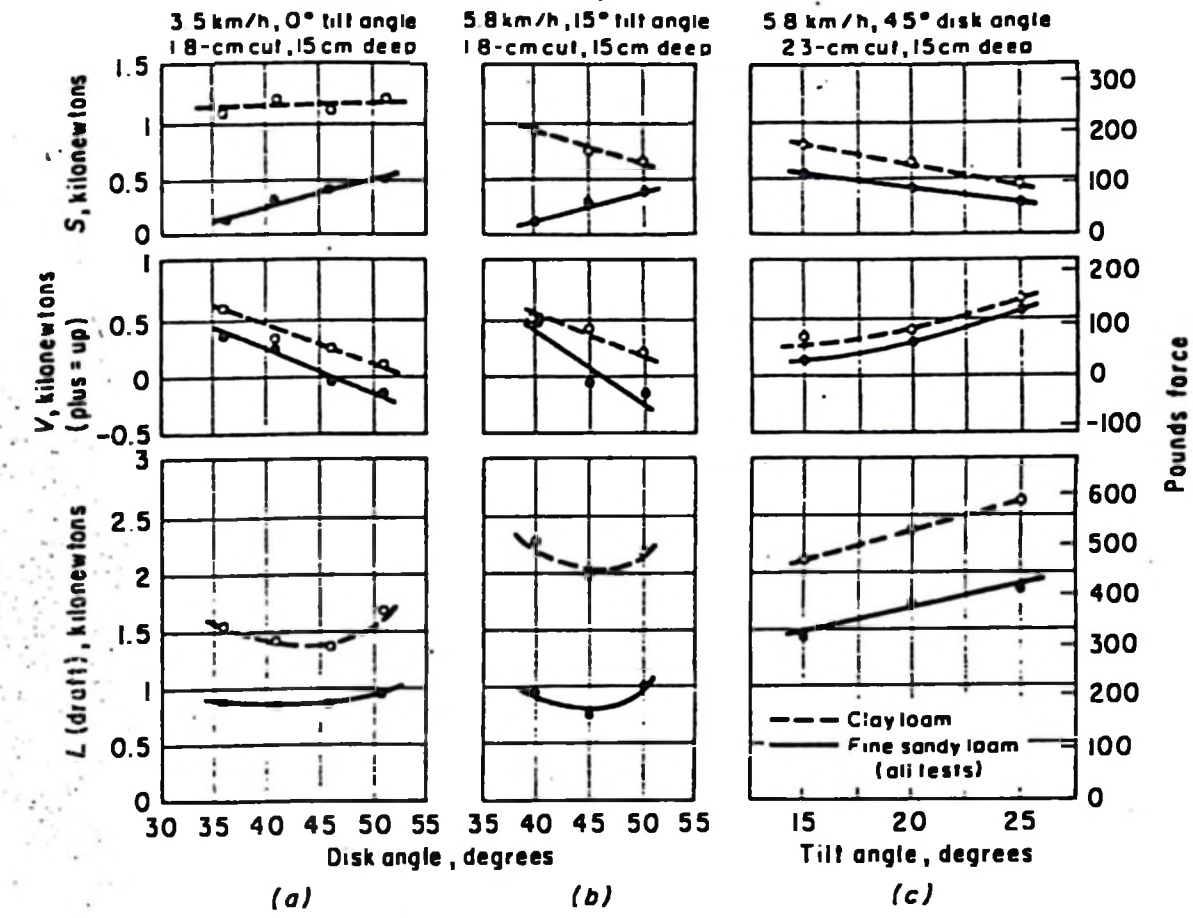

Figure 2.4. Soil reactions versus disc angle and tilt angle for a 660 mm disc having a 569 mm spherical radius of curvature (Gordon (9)).

2.2.2. Disc velocity

There is some slight variation of the draught and vertical forces when the speed of operation changes. Higher variations have been noticed in the side force, which may be due to accelerating the mass of soil sideways. As the speed increases, similarly the rate of change of momentum of soil mass sideways increases, which is responsible for the increase of the side reaction. This is supported by Newton's Second Law of Motion, " Rate of change of momentum is proportional to the applied force and takes place in the direction which the force acts."

For a disc angle of 45°, a tilt angle of 18 to 20°, a depth of 150 mm and a width of cut 180 mm and 230 mm, Gordon (9) found out that when speed was increased from 4.8 km/h to 9.6 km/h, the draft L increases 40 per cent in clay loam and 90 per cent in fine sand loam. The side force S also increased with speed because the soil is thrown further to the side.

The vertical upward force V decreased as speed was increased. Thus, with the blade tilted, increasing the speed would improve soil penetration under the soil conditions mentioned above.

From the results of Harrison (10), experiment as shown in the Table 2.1 below, when the speed increased from 5 to 6 km/h by 14 per cent, the draught, vertical and side forces increased slightly by - 1.34, 0 and 3.56 per cent respectively.

Gill et al (5) found out that at shallow angles, there were no great changes in draught because the component of velocity in the side direction is small, as shown in Figure 2.5 below. When angles are increased the draught force increases more rapidly under the influence of the side force which is responsible for the rate of change of soil mass momentum.

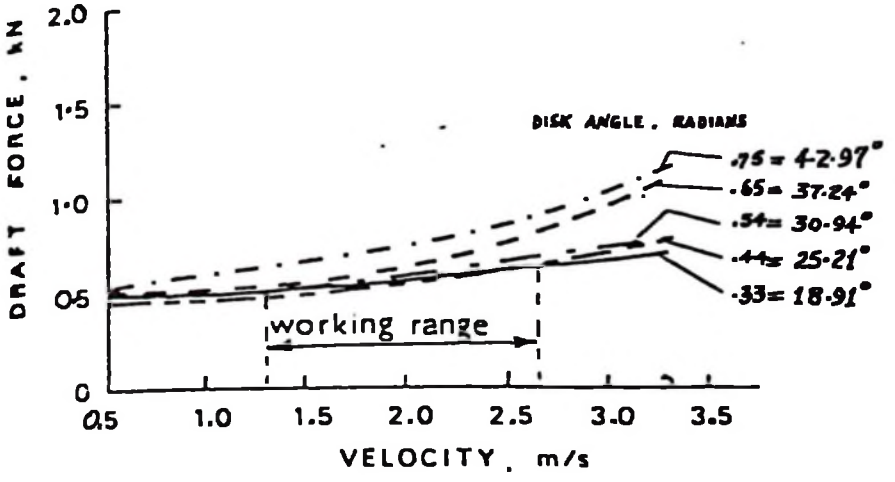

Figure 2.5. Relationship between velocity and draft with different disc angles (Gill et al (5))

	Draft	Vertical	Lateral
		(Newton per disc)	
Silty loam site	311	307	289
Clay loam site	449	347	480
51 mm depth	280	267	320
76 mm depth	180	387	449
5.6 km/h	374	329	365
6.4 km/h	369	329	378
7.2 km/h	387	329	387
8.0 km/h	396	329	405

Table 2.1. Soil reacting forces main effect (Harrison (10))

2.2.3. Disc geometry

Gordon (9) found out that the upward thrust of the soil increased with increase in concavity. A slight difference in draft in favour of the large disc was observed. Also,due to reduced upward thrust, the larger disc would tend to penetrate better. When the discs were inclined from the vertical position, the draft and penetration factors were reversed in favour of the smaller discs.

A comparison of notched and plain-edge discs showed slightly significant differences in draft and ability to penetrate the soil. However, when the discs were tipped back, the notched disc had the greater upward thrust.

Studies carried out by Gill et al (5) on harrow discs revealed that increasing the radius of curvature of discs,

coupled with selecting proper disc angle and mass on the disc, provide a means of making major changes in depth to which discs penetrate the soil.

The disc geometry parts which have some influence in the magnitude of forces are disc diameter D, its radius of curvature R and the sharpness of the cutting edge. According to studies done by Gill et al (5), the optimum range of disc shapes in terms of forces, were found to lie between discs of R/D ratios from 1.33 to 2.92. Increasing the radius of curvature, reduces the force on the back surface of the disc. A similar effect is caused by increasing the disc angle (from 12 to 20 degrees). The draught force is also reduced, which is an advantage to relatively lighter equipment operated at higher speeds with minimum power inputs. Proposed A.S.A.E. standards for disc blades are given below:

Disc diameter D	Concavity	Radius of curvature R
Harrows:		
406 mm (16 in)	38 mm (1½ in)	561 mm
457 mm (18 in)	44.5mm 1¾ in)	610 mm
508 mm (20 in)	50.8mm (2 in)	660 mm
Ploughs:		
610 mm (24 in)	84 mm (3¼in)	590 mm
660 mm (26 in)	90 mm (3½ in)	640 mm
710 mm (28 in)	95 mm (3¾in)	690 mm

Table 2.2. Proposed ASAE standards for disc blades (17)

2.2.4. Depth of cut

Various experiments have indicated that there are increases in draught, side and vertical forces as the

depth of cut increases to some extent. Experiments by Harrison on a 457 mm disc harrow indicate this (Table 2.1 and Figure 2.6).

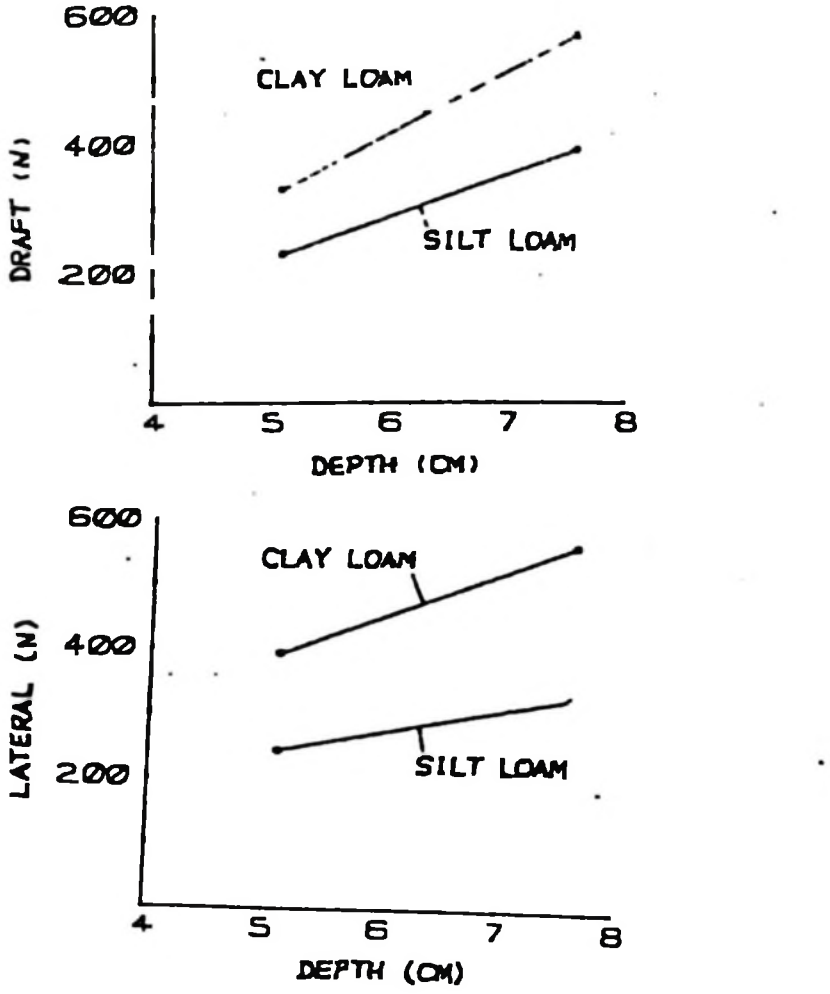

Figure 2.6. The effect of depth and soil type on draught and side forces (Harrison (10))

Similar indications were observed by Reaves et al(14) on different types of disc and of different diameters, the results are shown in Figure 2.7 for the draught and Figure 2.8 for the vertical reaction.

The variation of the side force with depth is influenced

by the disc angle. At low disc angles, 30 degrees, the side force changes from positive magnitude to negative as the depth increases. This is caused by the back pressure which builds up with depth. Back pressure is most effective at shallow angles, but at higher disc angles such as 45 degrees, the back pressure has little effect to counteract the soil reaction as the depth increases.

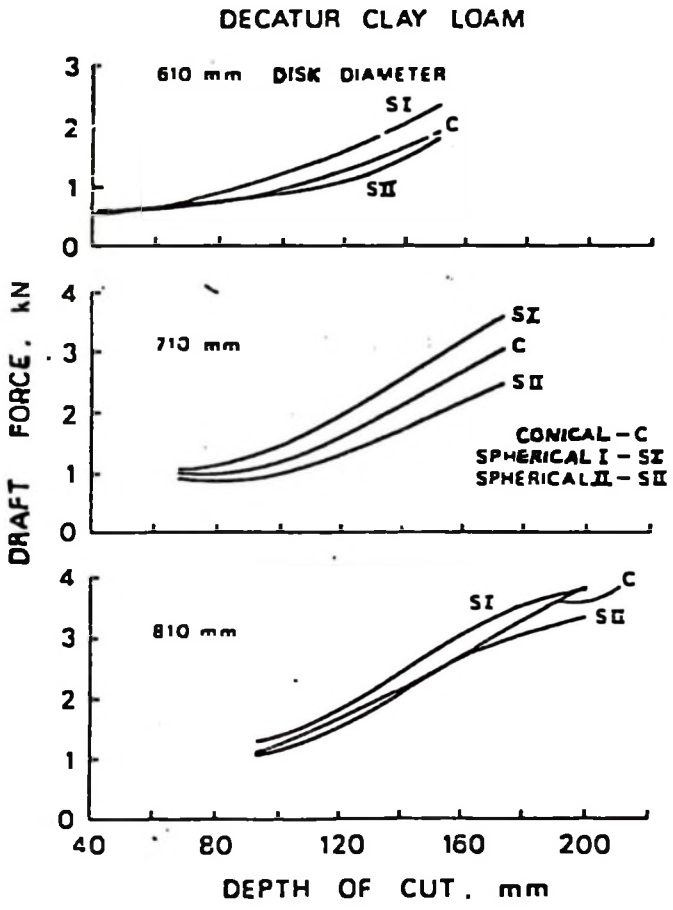

Figure 2.7. The effect of depth of cut on draught (Reaves et al (14))

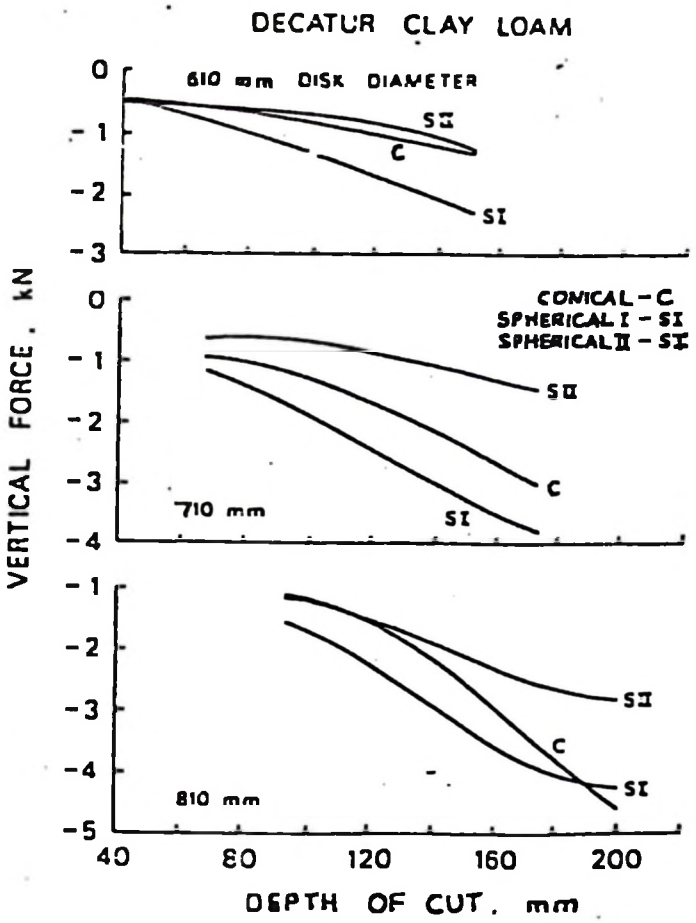

Figure 2.8. The effect of depth of cut on vertical reaction (14)

Field tests done by Taylor (17) in Australia revealed that when operating at 90 mm depth in sandy clay loam, L increased about linearly between disc angles 33½ and 55½ degrees. At a depth of 130 mm in a grey silt clay, L increased with disc angle when the width of cut was 200 mm, decreased with a 100 mm cut, and remained constant when the cut was 150 mm.

2.2.5. Width of cut

Spacing of the discs is generally of the order of 230 mm. Thompson and Kemp (18) found out that wider spacing gives better penetration and clearance, while narrower spacings give better pulverisation and more uniform soil disturbance.

Reaves, Gill and Bailey (14) conducted tests for disc

harrows and found out that closely spaced discs require shallow angles for their action to overlap in disturbing soil as compared to widely spaced discs. Overlap effect also can be influenced by the disc diameter and depth of cut. The overlap effect reduces both the draught, side and vertical forces as overlap is increased, but when reduced by increasing spacing it has a reverse effect. The test results concluded that:

(i) Draught forces responded to increases in width of cut but the rate of increase was small, hence width of cut can be increased with relatively low increases in draught.

(ii) The magnitude of the vertical force increases slightly with increases in width of cut, although the rate of change was small. Thus the width of cut can be varied only to influence the design weight of harrow, by increasing the spacing in reduction of the number of discs. Figure 2.9 (a) shows that draught gradually increased with increases in width of cut.

2.2.6. Added weights

Discs for primary cultivation are generally 610 mm or 660 mm diameter and carry weight in the range of 75 to 135 kg per disc. For secondary cultivation, diameters of 500 mm or less may be used with weights as low as 25 kg per disc.

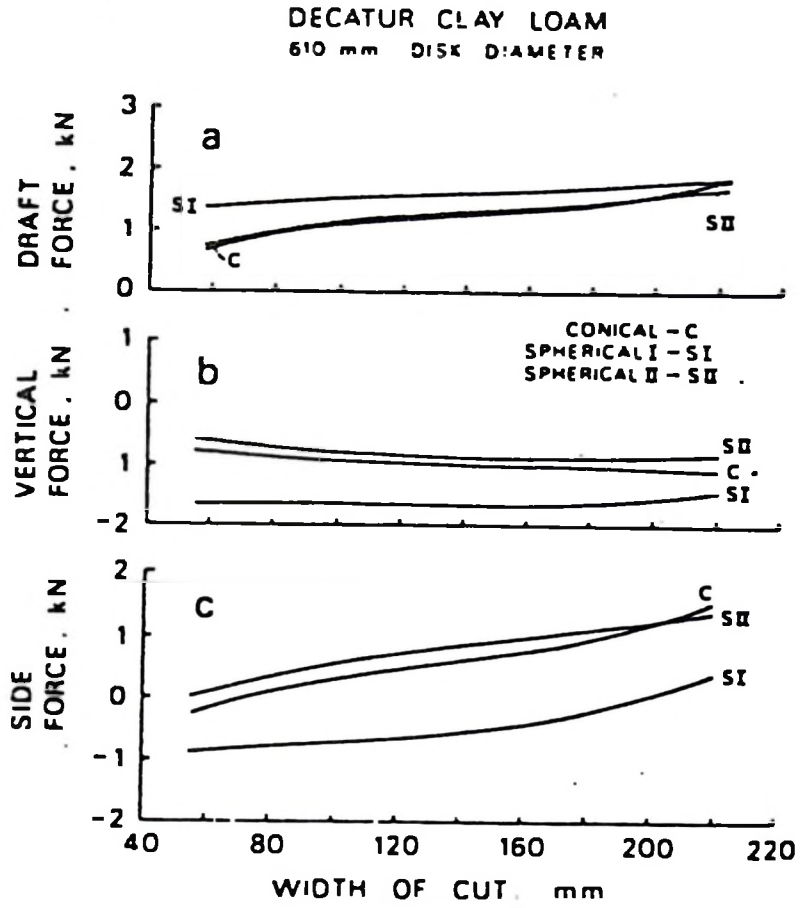

Figure 2.9. The influence of width of cut of 610 mm diameter discs on draft (a) and on the vertical (b) and side (c) forces in Decatur clay loams at a disc angle of 0.38 rad and velocity of 1.3 m/s (Reeves et al 1981,(14))

Weights are sometimes employed to overcome weight transfer at the rear gang and to counter balance the side force effect tending to lift the plough. Weights are also applied to improve penetration where the implement cannot do this by itself. However, increasing weight also increases the vertical reaction, which will influence the changes in draught and side forces. Increasing the working depth as a result of added weights will require higher draught forces, as discussed in previous sections.

2.2.7. Soil type

Depending on the shape and type of implement used, cutting or separation, shear failure, friction failure, compressive failure, or any combination of these may occur as the implement is forced into the soil. The resistance to penetration is usually considered to reflect the strength of the soil.

Pulling plough discs through a sandy loam soil and a fairly heavy clay soil has shown that soil type and conditions produced the most pronounced differences (9).

The characteristics of binding forces which are different in different soil types may have an influence on the variation of the forces required in different types of soils. The binding forces in clay types of soil are higher than those in silty and sandy types. Thus it requires higher forces to break clay types of soil than others. Some experimental results indicate this fact, as shown in Figure 2.6.

Soils with higher densities require higher draught and side forces. The side forces may respond to density because the rate of change of momentum is proportional to mass. Thus, soils with higher densities may involve higher draught forces which are influenced by the side forces. The density of clay loam shown in Figure 2.6 was higher than silt loam (mean density for clay loam was 1340 kg/m^3 and for silt loam 1260 kg/m^3).

2.2.8. State of moisture content

The presence of moisture in the soil weakens the bonding forces as its amount increases. Depending upon

tilth conditions, this phenomenon may help to reduce draught forces to be encountered. The relationship between soil shear strength and moisture content also exists, as shown in Figure 2.10.

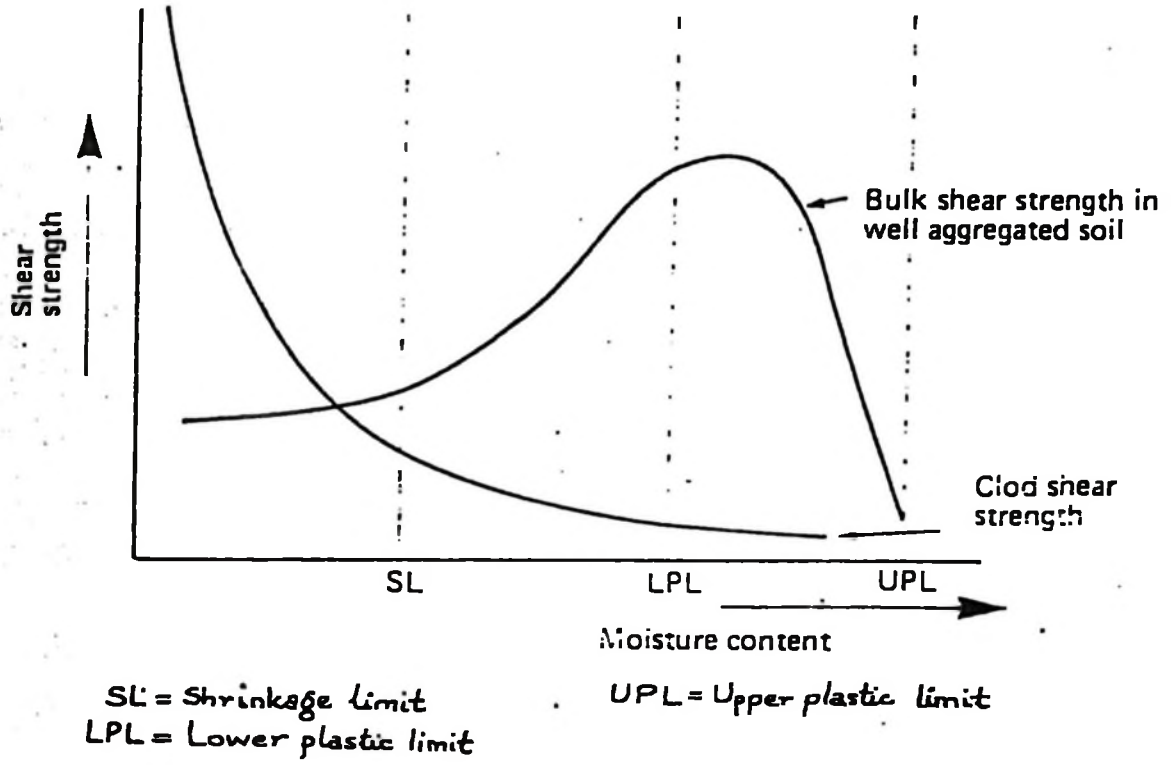

Figure 2.10. Variation in shear strength with moisture content (15)

An increase in moisture content causes an increase in density as shown in Table 2.3. This increase may be responsible for the increase of side force. However, the resulting effect will depend upon the factor which will be more dominant.

Soil	Block	Density kg/m³	Moisture content per cent (dry basis)
Silty loam	1	1240	40.7
	2	1310	44.2
	3	1250	35.0
	4	1240	32.2
	Mean	1260	38.2
Clay loam	1	1370	43.3
	2	1350	43.5
	3	1360	43.6
	4	1230	36.1
	Mean	1340	42.4

Table 2.3. The effect of moisture content on density (Harrison (10))

2.2.9. Rake angle

A disc plough can be considered as a wide tine angled sideways to the direction of travel. By changing the rake angle, the direction of the resultant disc force on the soil can be changed.

Payne and Tanner (12) found out that with rake angles of up to 45 degrees there is a downward component force assisting penetration. At greater angles the soil is opposing the implement's weight.

At rake angles below 50 degrees, the resultant force acts upwards and the smaller the rake angle, the greater the magnitude of the upward force. Between rake angles

of 40 and 70 degrees, the vertical force is small but its direction changes downwards as shown in Figure 2.11.

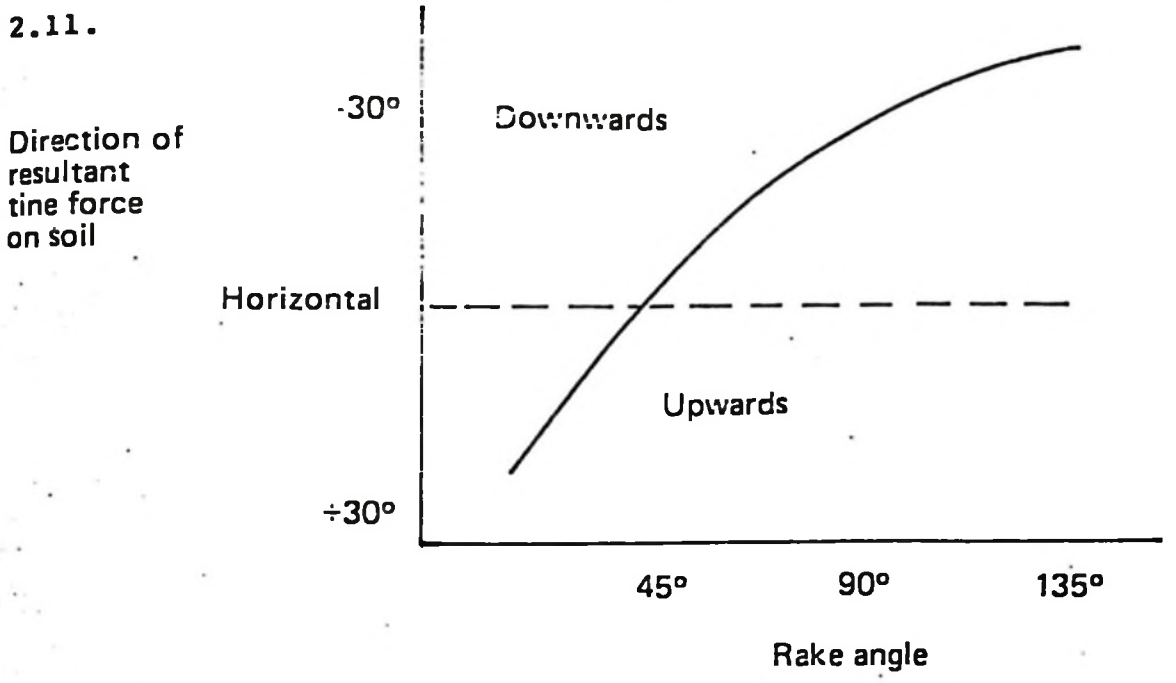

Figure 2.11. Change in direction of resultant disc force with rake angle (15)

The magnitude of the downward component increases rapidly with increasing rake angle above 90 degrees, reaching a maximum when soil force on the implement is equal and opposite to the above.

If penetration is required on hard, cemented soils, rake angles of 45 degrees or less should be used to make use of maximum downward soil force (15).

Rake angles also influence the magnitude of the horizontal or draught force on the tine as shown in Figure 2.12 below:

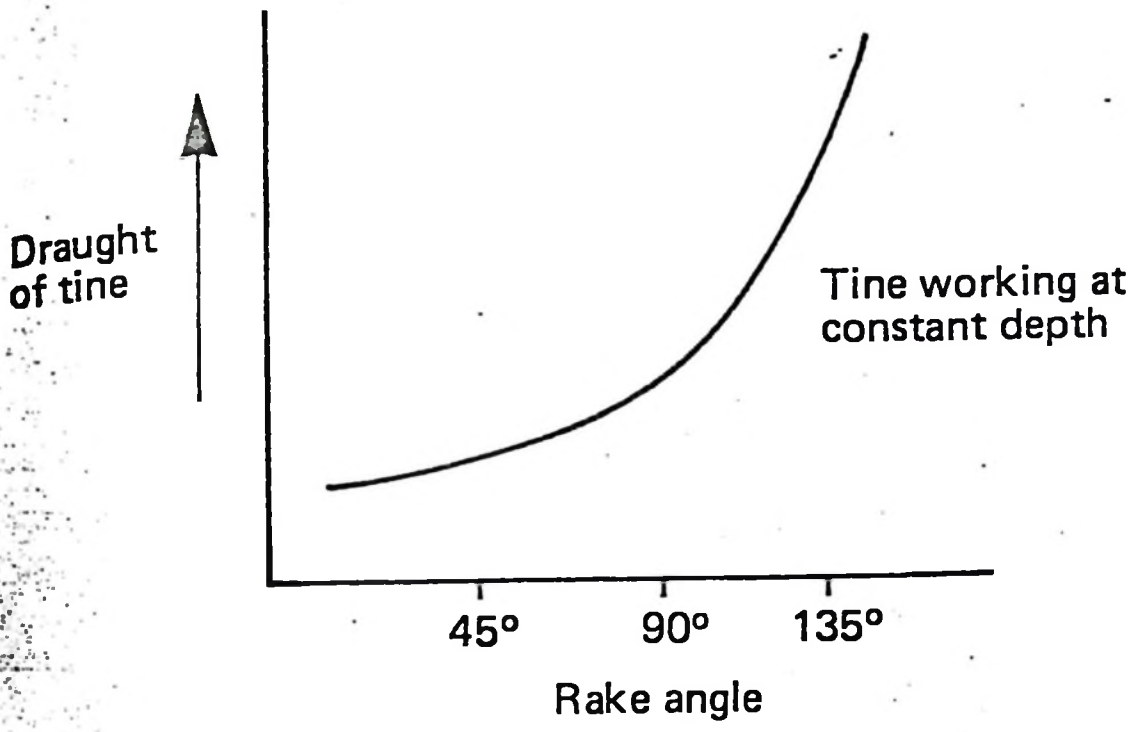

Figure 2.12. Effect of rake angle on draught (15)

From figure 2.12 above, it can be seen that not only does draught increase with increasing rake angle but the rate of increase becomes greater with discs of more than 50 degrees rake. To minimise draught, which is particularly important from a traction point of view, rake angles should wherever possible be kept below 50 degrees, provided the job required can be performed. Payne and Tanner (12) found out that the rate of increase of draught with rake angle becomes greater with rake angles of more than 50 degrees. A very much higher draught is experienced at rake angles greater than 90 degrees. From the theoretical point of view, it might be supposed that at both extremes of rake the draught would tend to infinity. This is obvious for rake tending to 180 degrees but is also likely to be true for rake angles tending to zero. The mechanism is similar to that for extreme "angles of sharpening" on vertical tines where the rise in area of soil interface more than offsets the drop in normal pressure (12).

3.0. METHODOLOGY

Prior to the start of the study, it was decided that the experiments should be conducted in the laboratory soil bin developed at the College. This was done to enhance homogenous conditions for each test run. Although the latter was not representative of the field conditions, the trend of the magnitude of the draught, vertical and side forces were expected to indicate whether the angling of the disc axis gave any improvement in penetration or not.

It was necessary to modify the existing disc attachment to enable the tilting of the disc axis. The tilting of the disc axis clockwise to the horizontal was done within the span of 0^{o} to 30^{o}. This gave rake angles of 65^{o} for 0^{o} axis to 35^{o} rake for 30^{o} axis angle.

Due to the limitations offered by the existing block, it was only possible to drill holes for 0^{o}, 5^{o}, 15^{0}, 20^{o} and 30^{o} axis angles. The intention was to increase the axis angle clockwise to the horizontal by steps of 5^{o}.

The span of 0^{o} to 30^{o} axis angle was chosen because it was suspected that the critical axis angle when the disc starts scrubbing would be between the two limits. A deep spherical disc was selected for the test because it is the common type used in the problem area mentioned in section 1.0.

The sweep angles of 90^{o} and 25^{o} were chosen for comparison of their effect on the magnitude of forces. A prediction model based upon Mohr-Coulomb soil mechanics theory and developed by Godwin and Seig (8) was used to

predict the draught, vertical and side forces and the predicted results were compared with experimental

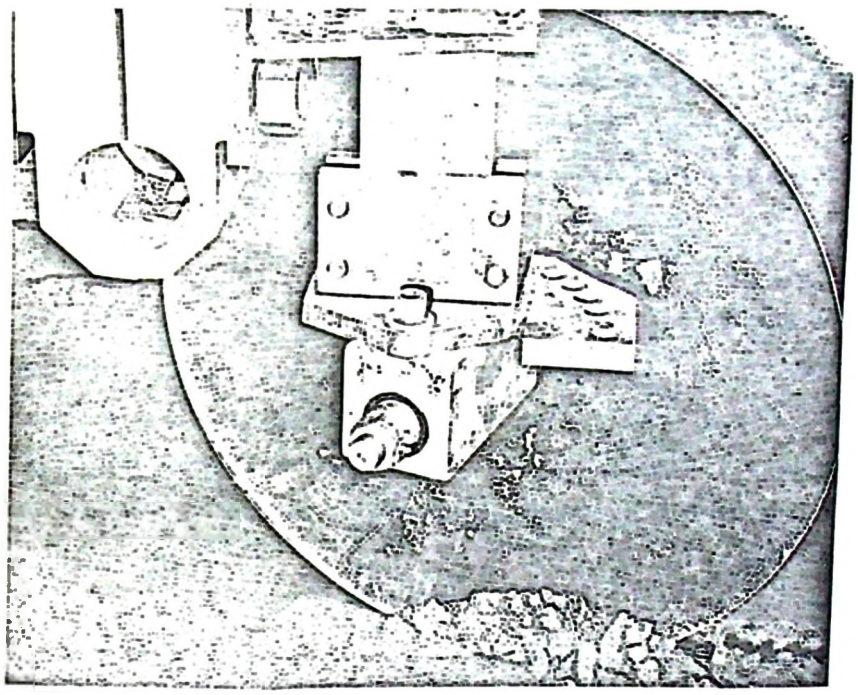

Plate 1(a) : The previous set-up of block before modification

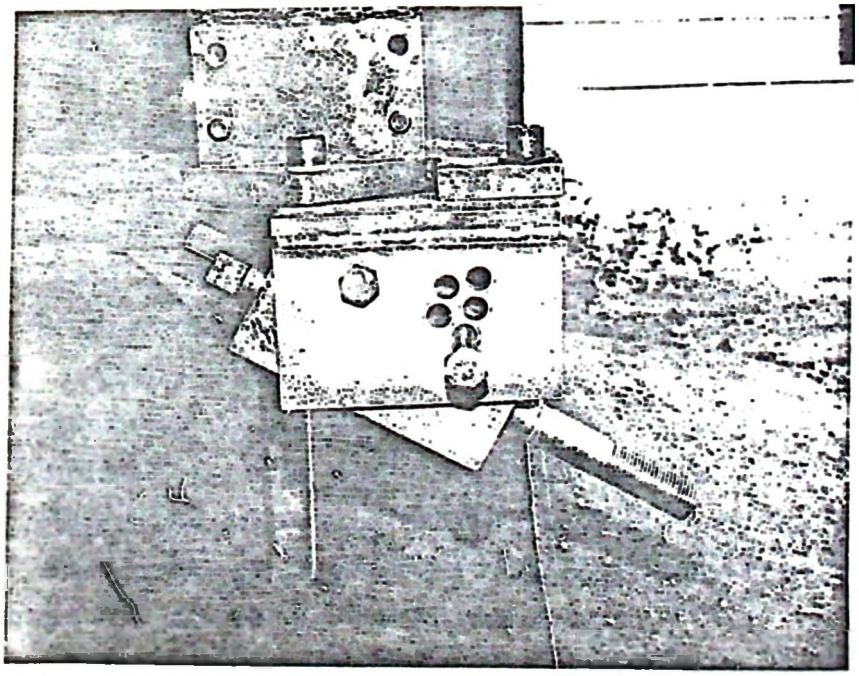

Plate 1 (b) : The set-up after modification

3.1. Design modification of existing equipment

To enable the use of the existing equipment, a U-shoe was designed and the existing block modified to facilitate the rotation of the disc axis. The modification is as shown on Plate 1(b). The previous block is as shown on Plate 1 (a). The alternatives to the above modification would have been:

a) Fabrication of wedge-shaped steel plates with respective axis angles. This proved unsuitable due to its limitations to adjustment of the working depth, especially at larger axis angles. It would also have demanded more time in changing the plates.

b) Modifying the disc attachment on a conventional plough. This would have involved using wedge-shaped plates, causing not only the problems mentioned in (a) but also that of matching of this modification with the existing set-up.

3.2. Description of equipment used

The set up of the apparatus used is as shown on Plates 2(a), 2(b) and 2(c). The draught and vertical force components of the resultant soil reaction were measured using the extended octagonal ring transducer and the side force measured using a strain gauged cantilever beam attached to the above transducer, as shown in plate 2(a). The disc was winched through the soil in the bin by the tractor operator. The instrumentation equipment is as shown on Plate 2(c).

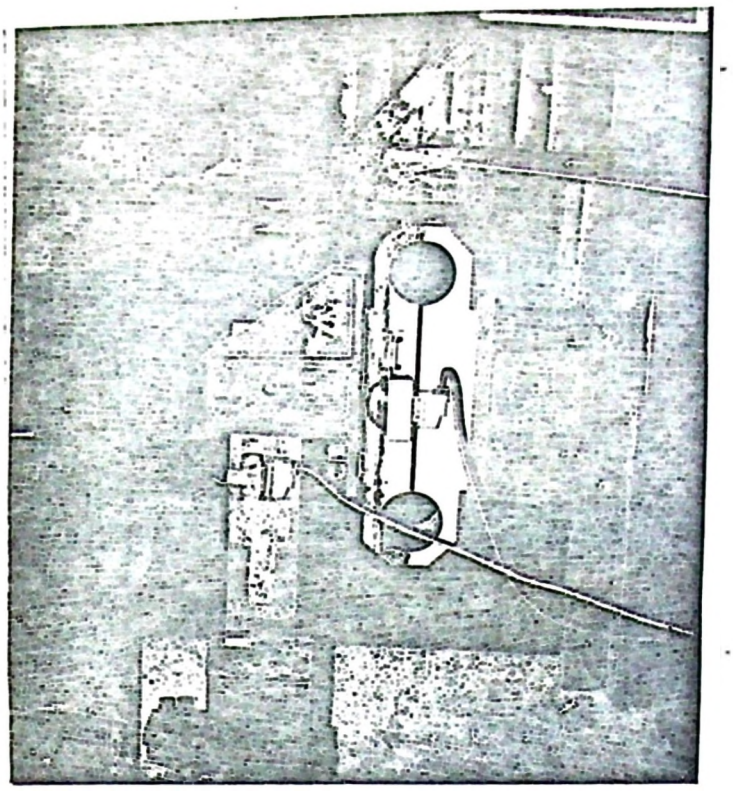

Plate 2 (a) : The force measuring equipment set-up

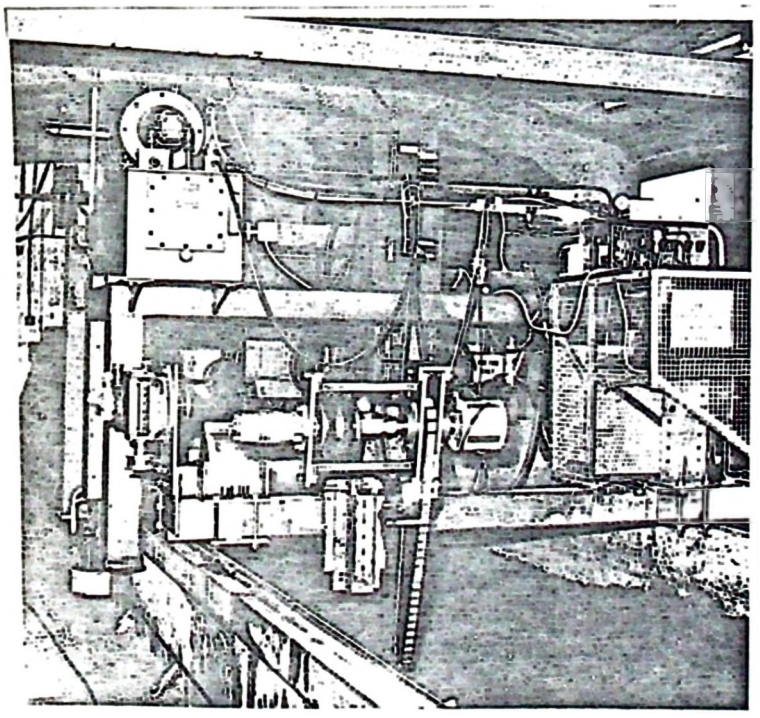

Plate 2 (b) : The soil handling and preparation equipment

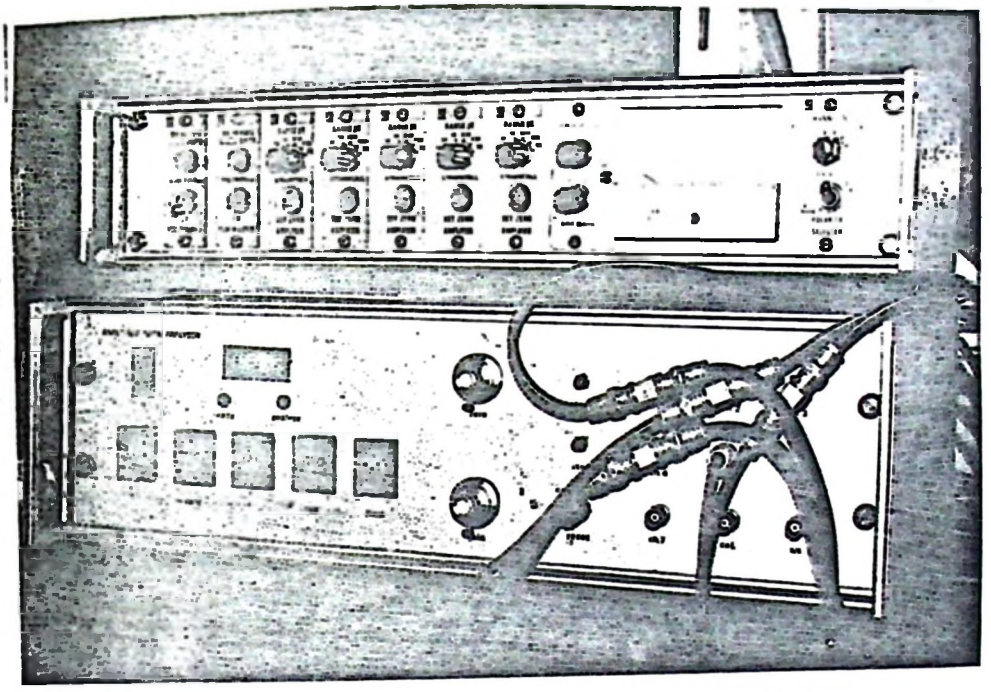

Plate 2 (c) : The instrumentation equipment

3.3. Pilot experiments

Preliminary runs had to be carried out to find out whether or not there was any limitation to the modifications made. The test revealed that some changes had to be made on the attachment of the disc leg to the carrier frame. These changes facilitated movement of the disc up or down to correct the working depth every time the axis angle and sweep angles were changed. The pilot experiments also revealed what magnitude of forces should be expected.

The results of the preliminary runs are shown in Appendix B.

3.4. Methods and experimental details

3.4.1. Transducer calibration

The determination of calibration constants was done at the outset of the experiments using static weights. The constants were determined when the transducer was used in conjunction with the amplifier. Units obtained from the recording equipment were analysed graphically, as shown in Appendix A, to find the calibration constants for draught, vertical and side forces. The circuits were calibrated prior to each test, using the shunt resistance as described by Godwin (7).

3.4.2. Moisture content, bulk density and soil preparation.

The soil used for this investigation was a sandy

loam. The moisture content was kept beteen 8% and 9% with an average of 8.6% for all the runs. The wet bulk density was 1.51 g/cc while the dry bulk density was 1.38 g/cc.

The bin was filled with soil to a level of 50 mm, levelled with the blade and then compacted using a pavement roller.

The surface was scratched with a scratching edge before a new layer was added. The process was repeated in 50 mm increments. The equipment for soil handling and preparation is shown on Plate 2 (b).

Upon completion of a test run the soil was removed in 50 mm layers by the blade and deposited in the final section of the soil bin. The soil was replaced using a grab on the carriage and the above process repeated.

At the end of the day's work, the soil was covered with a polythene sheet to reduce evaporation. Water lost was replaced before the start of the next day's runs. The application of water was done using a watering can. A fine and relatively even application was ensured on every 50 mm of soil layer for the first soil bin preparation.

3.4.3. Angle and depth setting

The modification as on Plate 2 (b) enabled the angling of the disc axis. For every run different axis and sweep angles were set. The angles were changed in an orderly manner. The runs were replicated three

times. The working depth was kept constant at 100 mm. Before every run was started, the depth was checked by winching the disc through the initial sections of the bin, pulling it out and measuring the depth. The depth was corrected by changing the position of the disc leg, i.e. moving it up or down.

3.4.4. Calibration of instrumentation equipment

Prior to each test, the reference zero and gain settings were checked for each channel of the amplifier unit, using the electrical calibration shunt resistances to give the relevant signal levels.

By pressing the start and stop buttons on the analyser, the data logger performs the analogue to digital conversion and the printer,which is connected to the analyser, as shown on Plate 2 (c) prints the bridge outputs. The outputs were then transformed to force units using the following formula:

$$\frac{\text{Bridge output}}{\text{Calibration value}} \times \text{calibration constant} \times 9.81 \text{ Newtons}$$

3.4.5. Speed selection and winching of the disc

The disc forward speed of 0.3 m/s (1.08 kph) was selected due to the short effective length of the bin. This enabled recording of bridge outputs at two positions in the bin as the disc was winched through the soil.

3.4.6. Data recording and depth measurements

As the disc was winched through the soil, the bridge outputs were recorded at two points of the bin. This was done by pressing in sequence the start and stop buttons on the analyser as the disc reached the points selected. The bridge outputs were printed by the printer.

The depth of work was measured at three points of the bin. This was done to ensure that the disc was working at the same depth for every run performed.

3.4.7. Moisture content and bulk density measurement

At the end of each run, soil samples were taken at three points of the bin, for moisture content determination. The mean moisture content obtained gave an indication of the percentage of moisture in the soil at a given time. This also showed whether or not the moisture content was kept within the same range.

The wet and dry bulk densities were determined by taking samples at three points on the undisturbed portion of the soil in the bin. The samples were then weighed, the volume of the container determined and wet bulk density calculated. The sample was then oven-dried and the dry bulk density determined. The summary of moisture contents and bulk densities is given in Appendix C.

3.5. Force prediction

Godwin and Seig (8) developed a force prediction model based upon the Mohr-Coulomb soil mechanics theory.

This model was used to predict the magnitude of the draught, vertical and side forces to be expected.

The formula used is shown below:

$$P = \frac{(\gamma_i \, d^2 \, N_\gamma + cdN_{ca} + (R-d) \, \gamma_f \sin\theta dN_q)}{2\sqrt{2Rd-d^2} \sin\theta}$$

where

P	= passive cutting reaction	kN
d	= depth of blade (assumed constant over complete width of disc)	m
γ_i	= initial bulk unit weight	kN/m^3
γ_f	= final bulk unit weight	kN/m^3
c	= cohesion	kN/m^2
q	= surcharge	kN/m^2

N_γ, N_{ca}, N_q } Dimensionless numbers given in Appendix D

l = effective width = $w \sin\theta$ where w is true width at the depth of soil cutting (d) and is given by

$$w = 2\sqrt{Rd-d^2} \sin\theta$$

The sample calculation and the summary of the force prediction is given in Appendix D.

4.0. RESULTS AND DISCUSSION

Figures 4.1, 4.2 and 4.3 show the reaction of draught, vertical and side forces to change in axis angle between 0^{o} and 30^{o} , at 90^{o} and 25^{o} sweep angles.

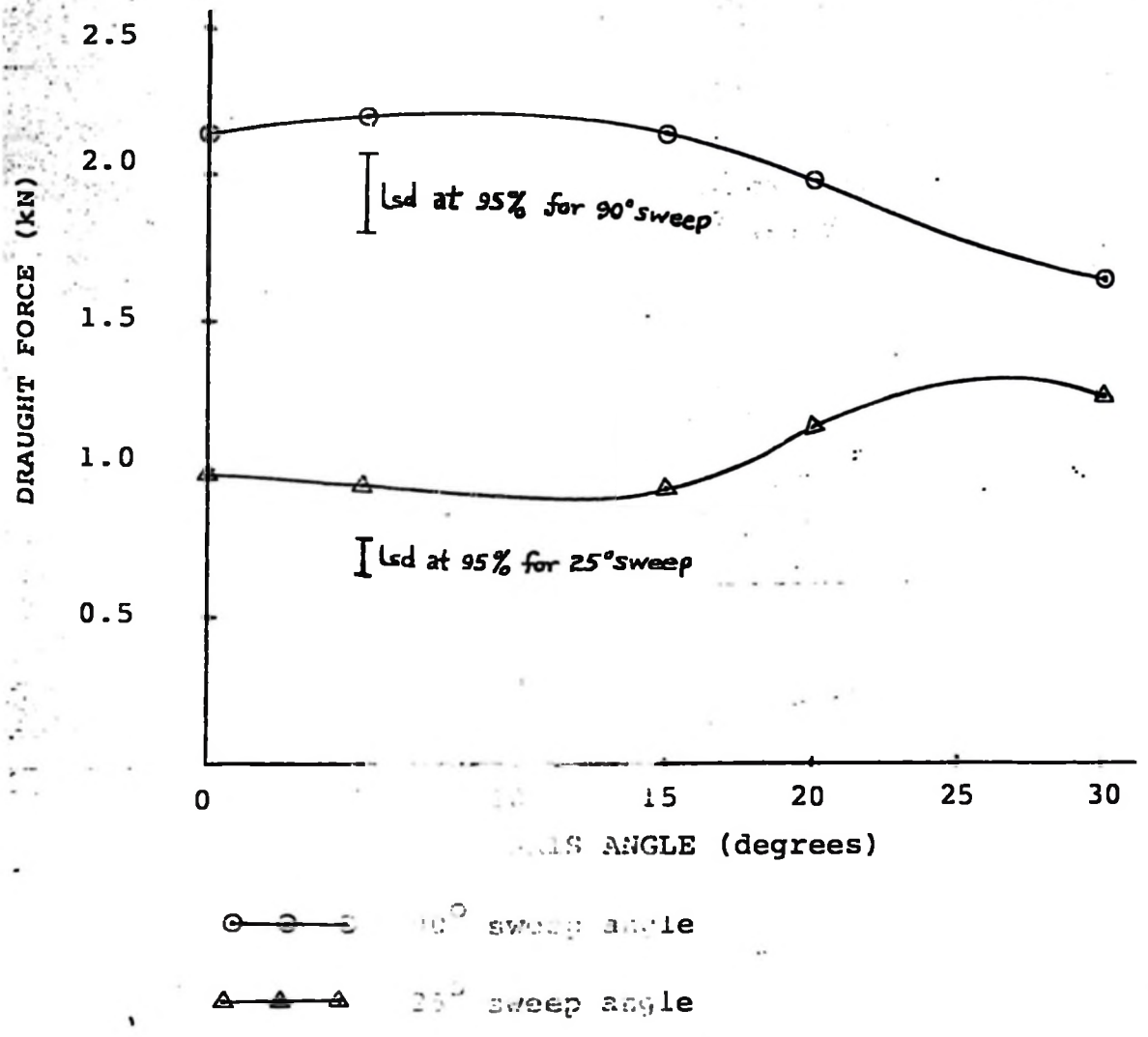

Figure 4.1. The reaction of draught force to change in axis angle for 90^{o} and 25^{o} sweep angles.

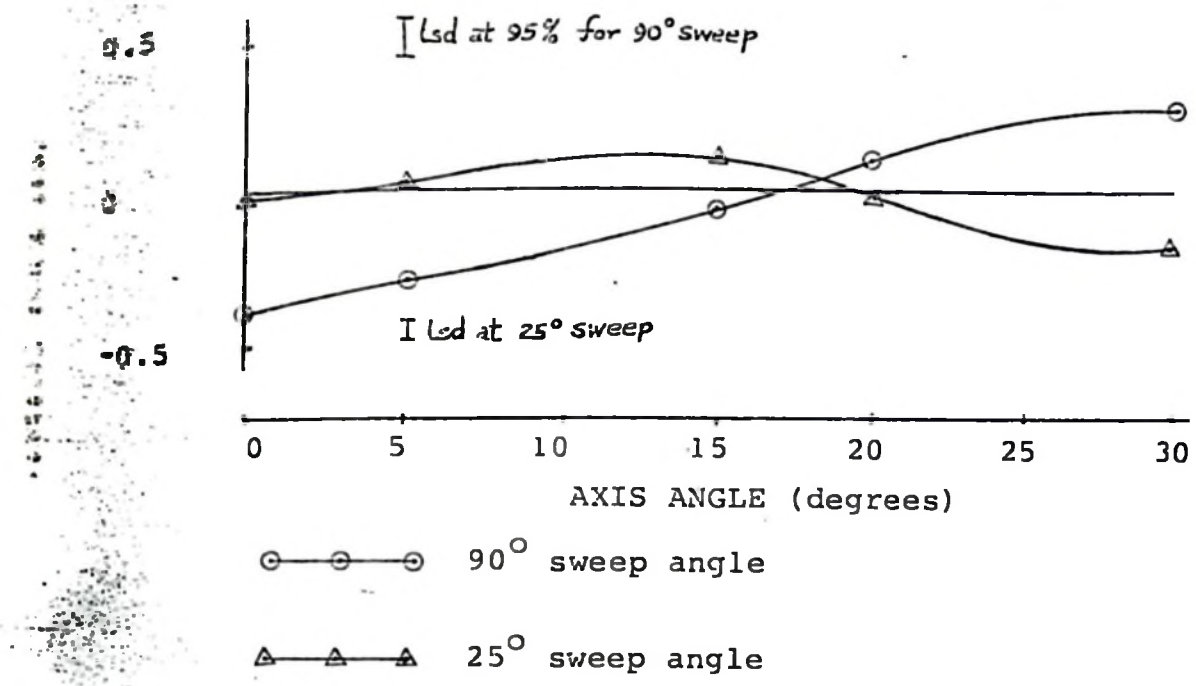

Figure 4.2. The reaction of vertical force to change in axis angles for 90° and 25° sweep angles

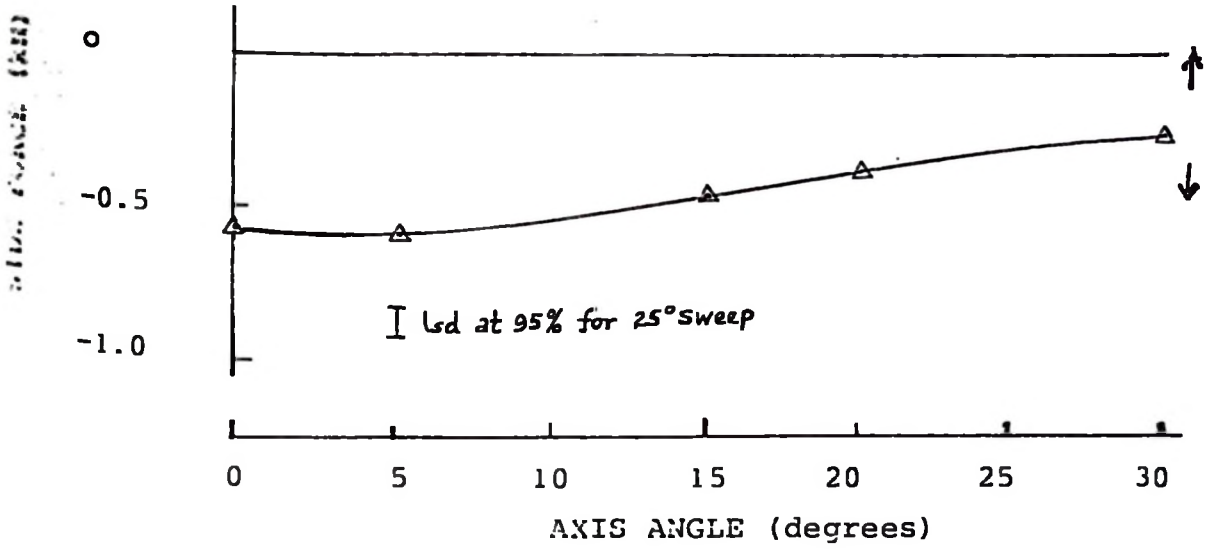

Figure 4.3. The reaction of side force to change in axis angle for 25° sweep angle

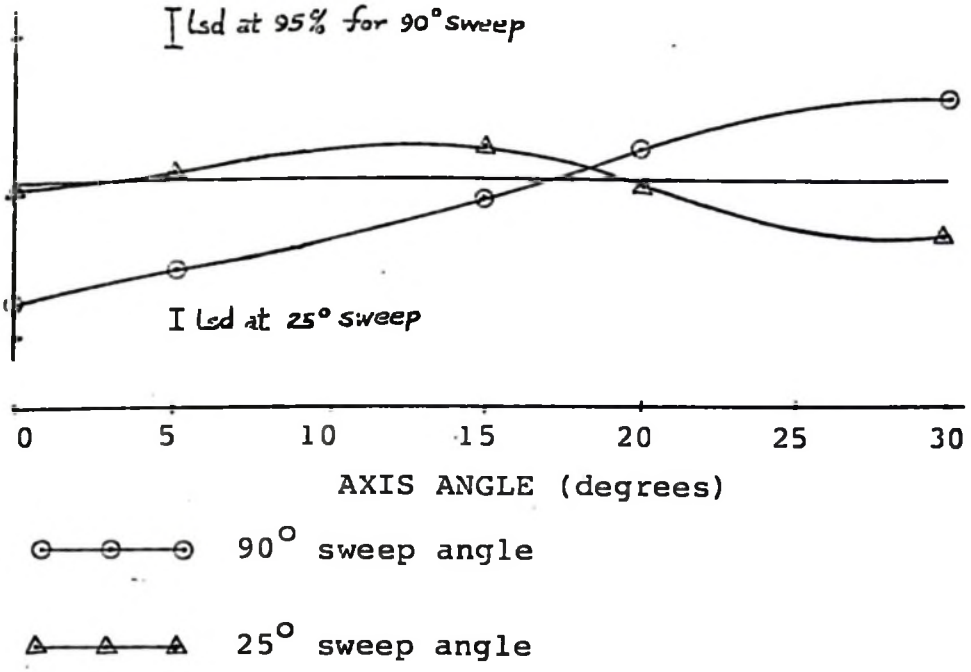

Figure 4.2. The reaction of vertical force to change in axis angles for 90° and 25° sweep angles

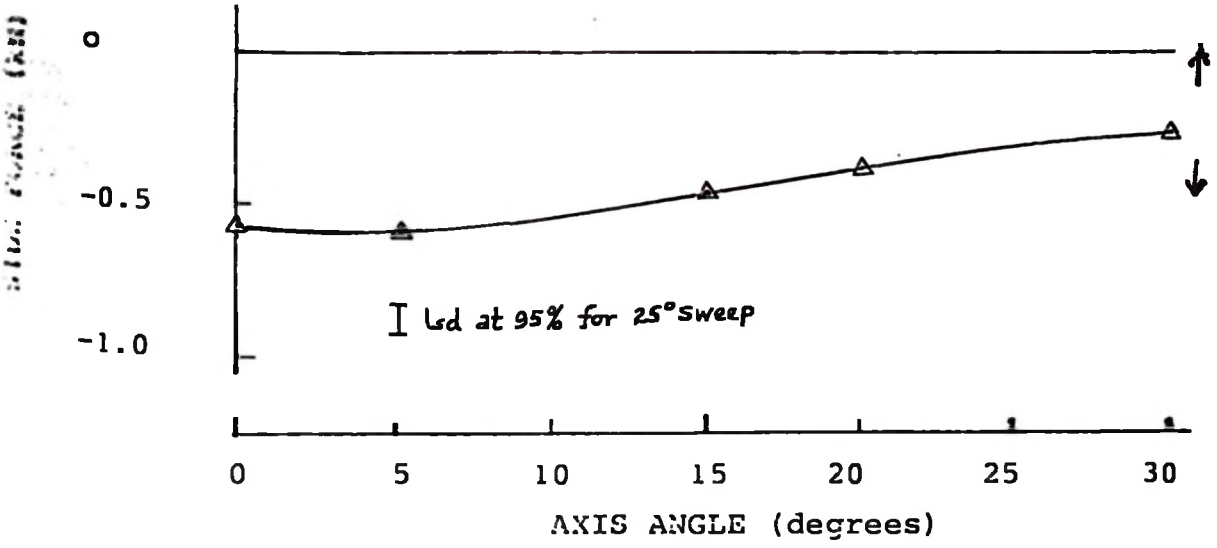

Figure 4.3. The reaction of side force to change in axis angle for 25° sweep angle

4.1. Analysis of results

The experimental results as summarised in Appendix E were analysed statistically (refer figures 4.1 to 4.3). In the analysis of variance (Appendix F) the effect of change in axis angle tested significant for draught and vertical forces at 90° and 25° sweep angles. It also tested significant for side force at 25° sweep angle. The test was carried out for 5% and 1% levels.

The least significant difference (lsd) test showed that at 90° sweep angle there was a significant effect between 20° and 30° axis angles for draught force, and between 5° and 20° axis angles for vertical force.

At 25° sweep angle the lsd test showed that the significant effect was between 15° and 20° axis angles for draught force and between 5° and 30° for vertical and side forces.

4.2. The reaction of disc forces on changes in axis angle

The graphical presentation of experimental results is given in figures 4.2, 4.2 and 4.3. The reaction of draught, vertical and side force is discussed below.

4.2.1. Draught force

For 90° sweep angle, the draught force decreased as the axis angle increased. The decrease was more pronounced between 20° and 30° axis angles. This reaction may be due to increase in bearing capacity area of the disc. The

rake angle effect may also influence this reaction. The rake angle decreases as the axis angle increases. This ties up with the findings of Payne and Tanner (12) that draught decreases as rake angle decreases.

In figure 4.1 the draught force at 25^{o} sweep angle seemed to decrease slightly up to 15^{o} axis angle and increased thereafter. The increase was more pronounced between 15^{o} and 20^{o} axis angles. The increase was probably due to increased scrubbing from the disc. The scrubbing effect seemed to decrease slightly as axis angle approached 30^{o}.

4.2.2. Vertical force

As shown in figure 4.2, at 90^{o} sweep angle the upward reaction (-ve sign) decreased steadily to beyond 15^{o} axis angle when the downward reaction (+ve sign) started to build up. This agreed with the findings of Payne and Tanner (12) and that of Spoor (15) who found that with rake angles of up to 45^{o}, there is a downward component force assisting penetration.

At 25^{o} sweep angle, the magnitude of downward reaction increased up to 15^{o} axis angle when it started to decrease. At about 20^{o} axis angle, the upward reaction started to build up. This was probably due to increased scrubbing from the disc.

4.2.3. Side force

There was no reaction of side force at 90^{o} sweep angle. This was obvious since the disc was symmetrical.

Figure 4.3 shows that at 25^{o} sweep angle the side force decreases with increase in axis angle. This agreed with the findings of Gordon (9) who found that increase in disc tilt angle decreased the measured side force.

The increase in bearing capacity area as the axis angle increased may be another reason for the decrease in side force.

4.3. A comparison of experimental and predicted results

A model developed by Godwin et al (8) was used to predict the disc forces. The Summary is given in Appendix D.

A graphical comparison between the predicted and experimental results is presented in figures 4.4 and 4.5.

4.3.1. Draught force

In figure 4.4, the experimental and predicted results did not compare well. The trend of action of forces at 90^{o} sweep angle was similar but the magnitudes differed.

At 25^{o} sweep angle the trend differed greatly. This is more prounced at axis angles about 15^{o}. Within limits of experimental errors, the variation was great. Time did not allow for repetition of the experiment or close examination of the force prediction model.

4.3.2. Vertical force

Figure 4.5 shows that the trend of action of

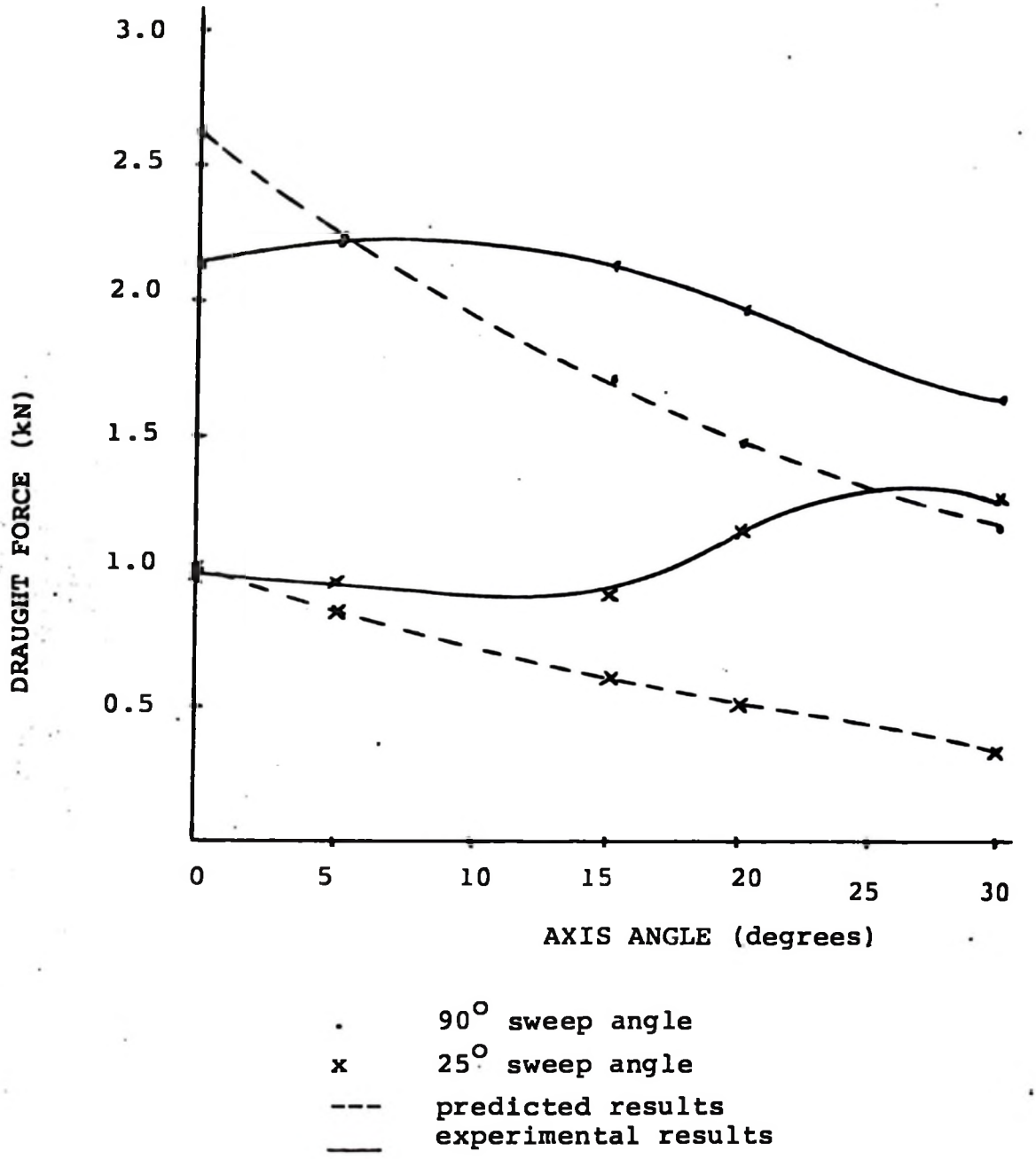

Figure 4.4. Comparison of experimental and predicted draught force.

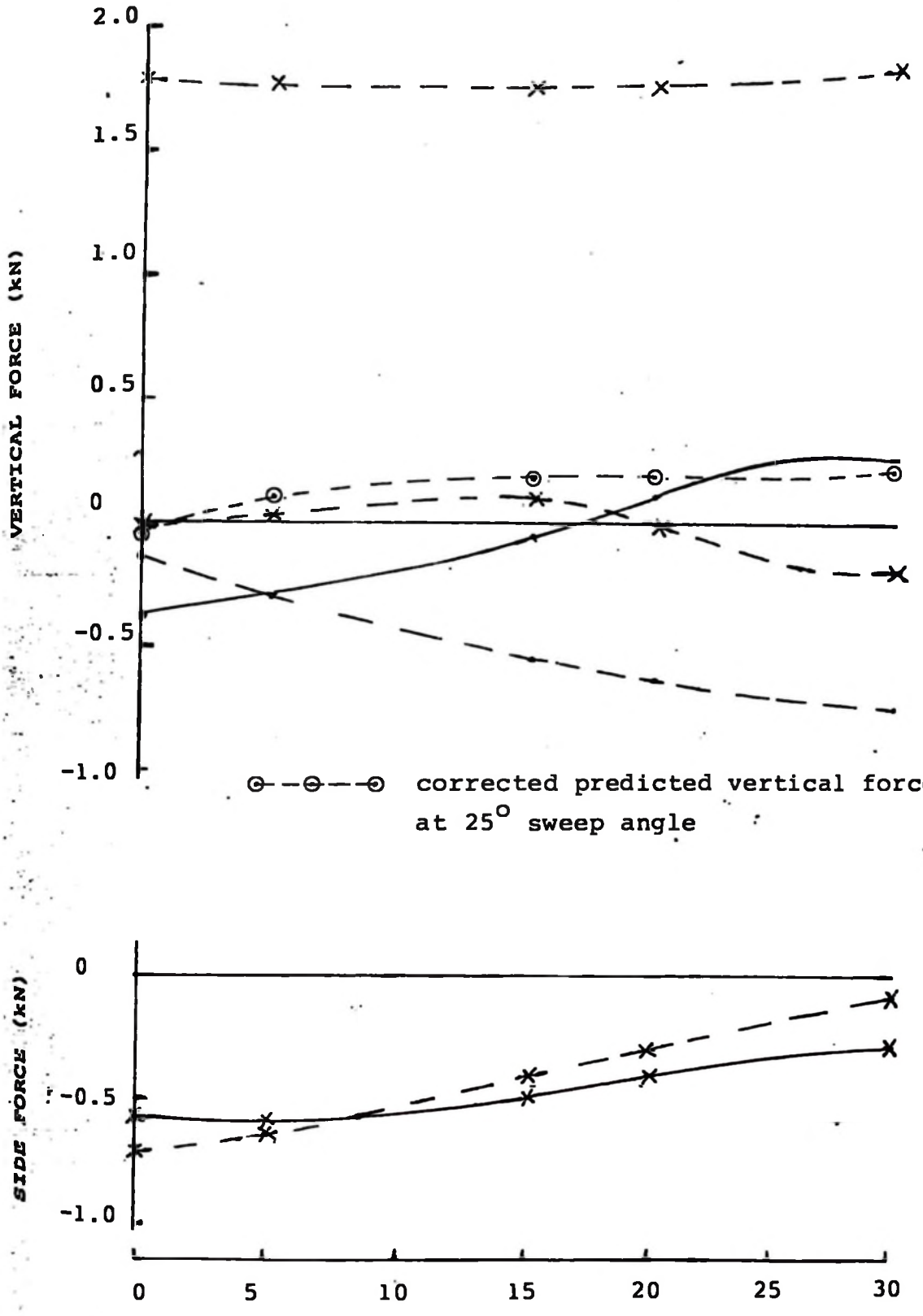

Figure 4.5 Comparison of experimental and predicted vertical and side forces (see figure 4.4 for key).

experimental vertical force compared fairly well with the predicted at 90° sweep angle. At 25° sweep angle the variation was too great in magnitude.

It seemed that some improvement could be made by considering the chamfer edge area in calculating the rear scrubbing forces. However, this could not improve the draught and side forces prediction. (See table 4.1 below):

Axis angle (deg)	Rake angle (deg)	Chamfer area $10\ m^2$	Predicted force (kN)		Experimental force (kN)
			Previous	Improved	
0	65	5.14	1.78	0.04	0.01
5	60	5.38	1.77	-0.10	-0.03
15	50	6.08	1.75	-0.18	-0.11
20	45	56.59	1.76	-0.20	-0.01
30	35	8.12	1.86	-0.23	-0.18

Figure 4.1. Comparison between predicted (improved) and experimental vertical force at 25°

4.3.3. Side force

Within limits of experimental errors the predicted and experimental forces compared fairly well.

4.4. Achievement of experimental objectives

The results showed that improvement in penetration could be achieved by changing the disc axis orientation. A suitable axis angle seemed to be between 15° and 20° where draught force and upward component of vertical force was minimum at 25° sweep angle. The side force was also decreasing between the two axis angles.

If time had allowed, it would have been quite helpful to explore the effect of using different sweep angles with changes in axis angle.

It would have been a considerable advantage to explore the reasons for the differences in experimental and predicted results, but time was the limiting factor. However, the results obtained may help in considering whether there is need to explore the force prediction model.

5.0. CONCLUSION AND RECOMMENDATIONS

The change in axis angle has a significant effect on draught, vertical and side forces. The change in sweep angle seems to be an important parameter in amplifying the effect. The exploration of an optimum combination of sweep and axis angles in improving penetration may be a useful venture.

The maximum downward vertical force occurs at smaller axis angles as the disc is swept from 90^{o}. The draught and side forces are also less at 15^{o} than at 0^{o} axis angle. The optimum axis angle at 25^{o} sweep is about 15^{o}.

An investigation on the effect of change in axis angle for different shapes and sizes of disc is recommended to determine optimum geometric parameters.

It would be of much interest to explore the prediction model to determine the reason for the difference between the predicted and experimental results. Whilst for global prediction the model seems alright, it is difficult to make it work for all combinations. The model works well with a 0^{o} axis angle and 90^{o} sweep angle. The edge effects and inclinations for the other combinations need greater definitions.

REFERENCES

1. Clyde, A.W. (1939). Improvement of disc tools. Agric. Eng. 20 (6): 215-221

2. Clyde, A.W. (1944). Technical features of tillage tools. Pennsylvania Agric. Experimental Station. Bulletin 465 (Part 2).

3. Gill, R.W. and Vanden-Berg, G.E. (1968). Soil dynamics in tillage and traction. USDA, Washington D.C.

4. Gill, R.W. and Reaves, C.A. (1980). The effect of geometric parameters on disc force. Trans. ASAE 23(2) 266-269, 274.

5. Gill, R.W. et al (1981). The influence of harrow disc curvature on forces. Trans. ASAE Vol.24 pp 579-583.

6. Gill, R.W. et al (1982). Harrow disc curvature - Influence on soil penetration. Trans. ASAE 25(5) : 1173-1180.

7. Godwin, R.J. (1974). An investigation into the mechanics of narrow tine in frictional soil. A PhD thesis. University of Reading.

8. Godwin, R.J. and Seig, D.A.T. (1984). Development and evaluation of a force prediction model for agricultural discs. Silsoe College. Unpublished.

9. Gordon, E.D. (1941). Physical reaction of soil on plough discs. Agric. Engr. 22 (6) : 205-208.

10. Harrison, H.P. (1977). Soil reacting forces for discs from field measurements. Trans. ASAE Vol. 20 pp 836-840.

11. Kepner, R.A. et al (1982). Principles of Farm Machinery. 3rd ed. The AVI Publishing Co. Inc., Westport, Connecticut, U.S.A. pp 160-166.

12. Payne, P.C.J. and Tanner, D.W. (1959). The relationship between rake angle and the performance of simple cultivation implements. Journal of Agric. Eng. Res. Vol. 4. pp 312-325.

13. Proposed ASAE Standard: Disc blades for disc plows, harrows, drills, listers and cultivators. The Journal of ASAE Vol. 20, No. 6, 1939.

14. Reaves, C.A. et al (1981). Influence of width and depth of cut on disc forces. Trans. ASAE Vol. 24 pp 572-578.

15. Spoor, G. (1975). Fundamental aspects of cultivation, soil physical conditions and crop production. H.M.S.O., London. pp 128-144.

16. Steel, R.G.D. and Torrie, J.H. (1960). Principles and procedures of statistics. McGraw-Hill Book Co. Inc. New York.

17. Taylor, P.A. (1967). Field measurements of forces and moments on wheatland plough. Trans. ASAE 10(6): 762-768, 770.

18. Thompson, J.L. and Kemp, J.G. (1958). Analysing disc cuts graphically. Agr. Engr. 39(5) 285-287.

APPENDICES:

APPENDIX A : TRANSDUCER CALIBRATION

(i) Draught force:

Weight (kg)	Calibration 1.	Calibration 2.	Calibration 3
	Run Values (Units)		
0	0	0	0
20	2	2	1
40	4	4	3
60	6	6	5
80	8	8	7
100	10	11	10
120	12	12	12
140	15	15	14
160	17	17	16
180	19	19	19
200	22	21	21
220	24	23	23
240	26	26	25
260	29	28	27
280	31	30	29
300	33	32	31

Table. A.1. Calibration of draught force

Channel gain : 1K
Calibration Unit : 98
Calibration Constant : 920 kg = 8.85 kN (From Figure A.1)

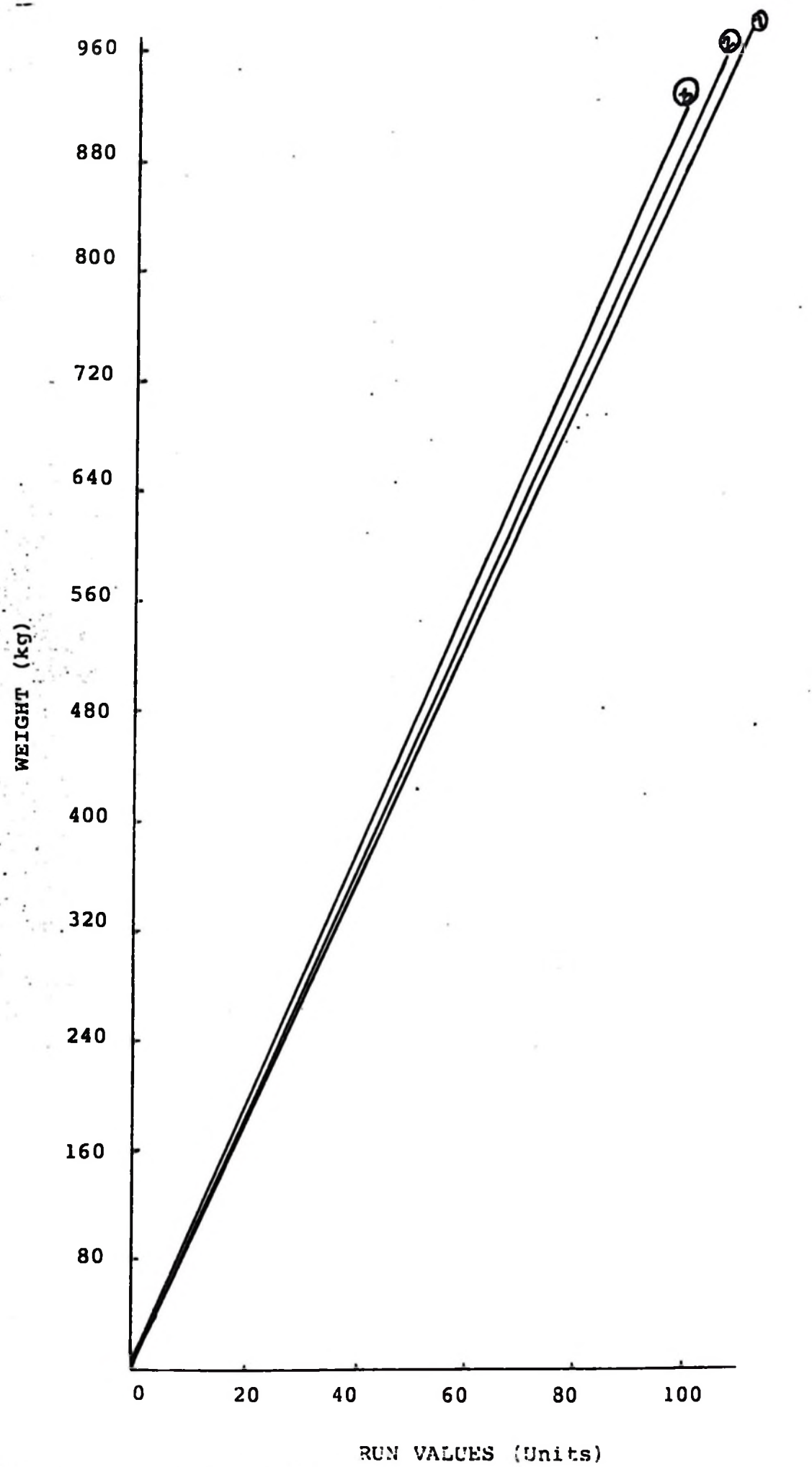

Figure A.1. Dreadnought force calibration

(ii) Vertical force:

Weight (kg)	Calibration 1	Calibration 2	Calibration 3
	Run Values (Units)		
0	0	0	0
20	6	6	6
40	14	14	14
60	22	21	21
80	29	28	28
100	36	36	36
120	44	43	43
140	51	51	51

Table A.2. : Calibration of vertical force

Channel gain : 300
Calibration unit : 101
Calibration Constant : 272.996 kg = 2.68 kN (From Figure A.2

(iii) Side force:

Weight (kg)	Calibration 1	Calibration 2	Calibration 3
	Run Values (Units)		
0	0	0	0
20	6	6	7
40	12	12	12
60	18	18	19
80	24	24	25
100	31	31	31
120	37	37	37
140	43	43	43
160	49	49	50
180	55	55	56
200	62	62	62

Table A.3 : Calibration of side force
Channel gain : 300 Calibration Unit : 102
Calibration Constant : 330.308 kg = 3.24 kN (From Figure A.3

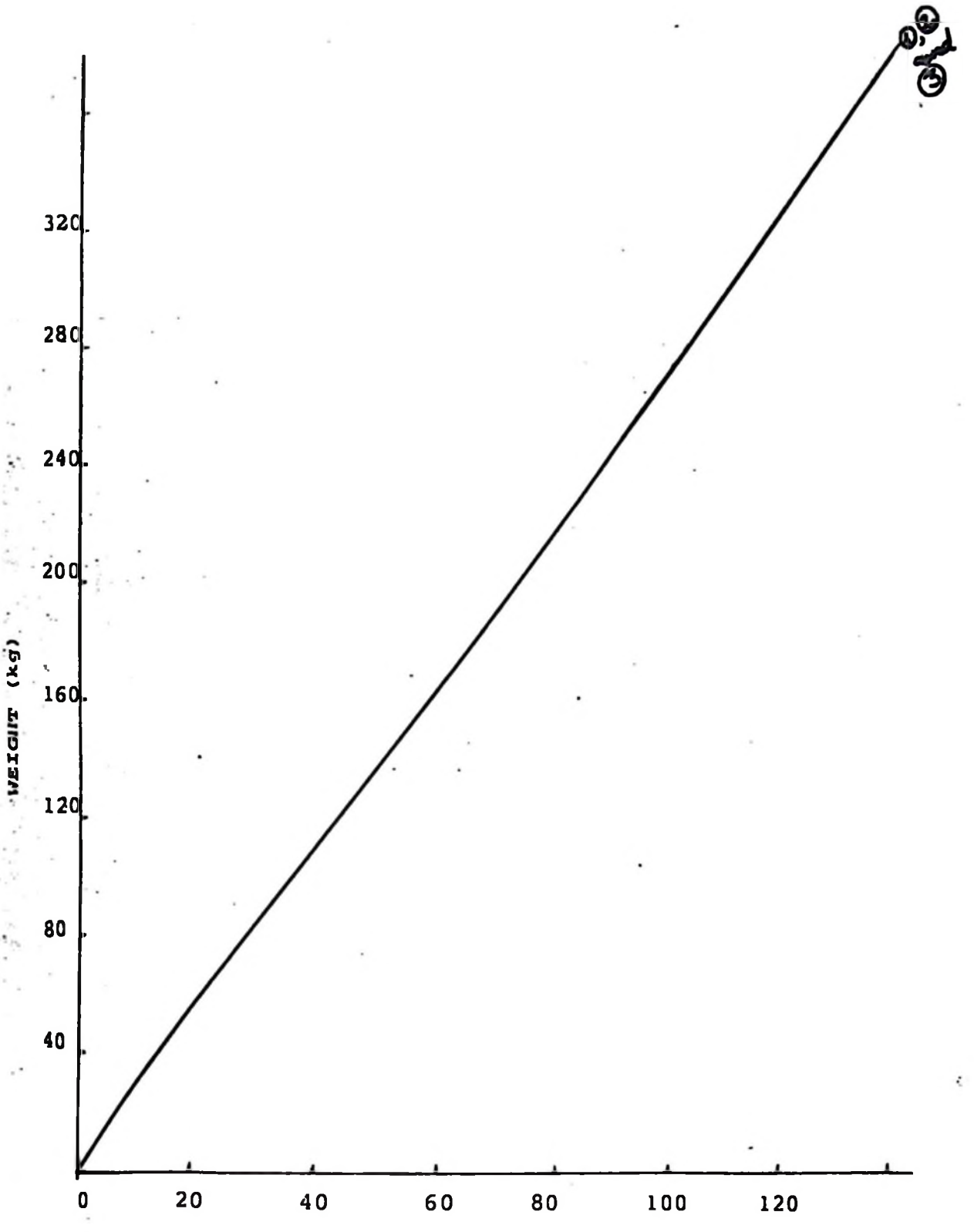

Figure A.2. Vertical force calibration

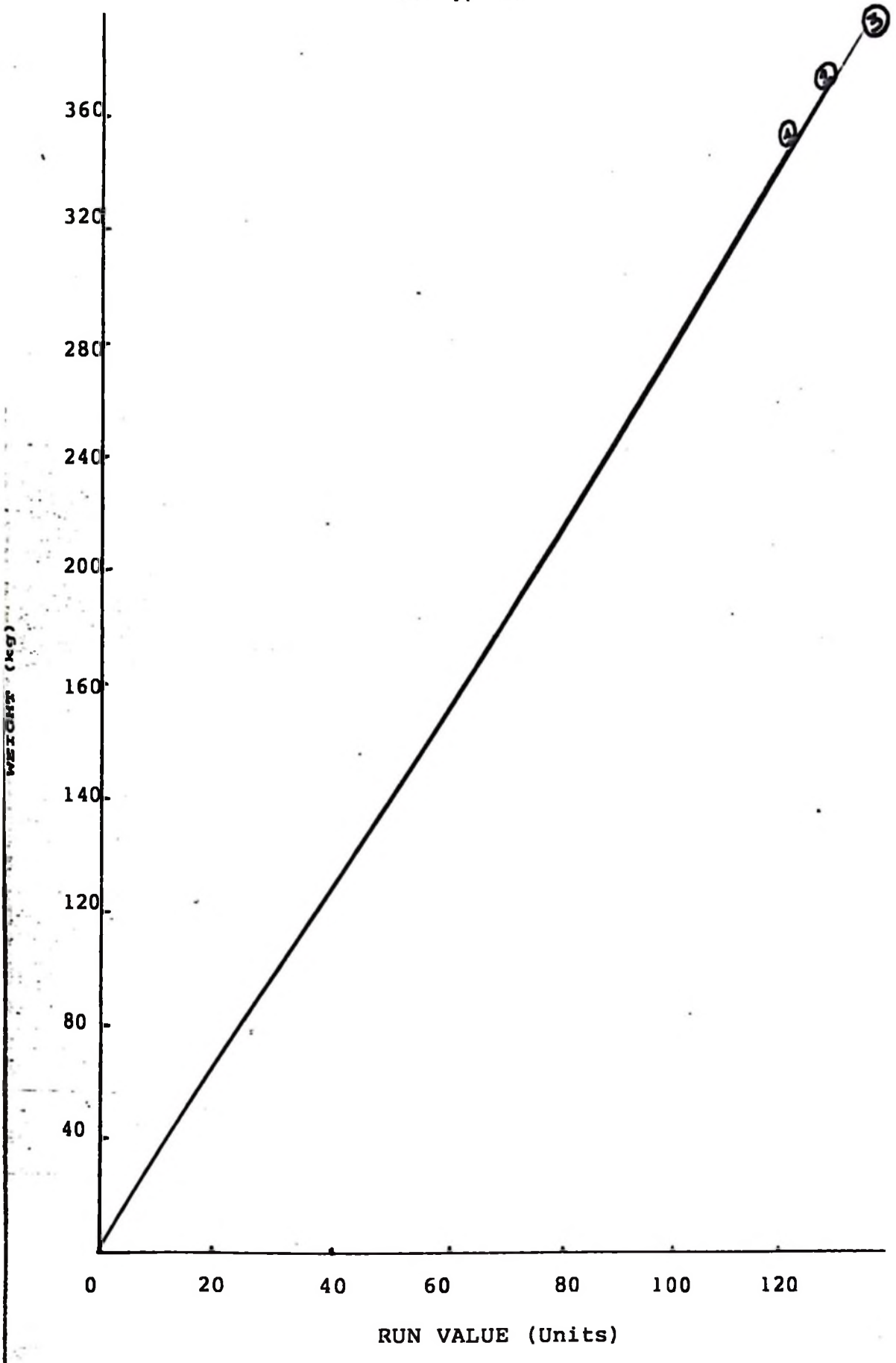

Figure A.3 Side force calibration

APPENDIX B : SUMMARY OF RESULTS FROM PRELIMINARY EXPERIMENTS

Sweep angle (deg.)	Axis angle (deg.)	Average Force (kN) Draught	Vertical	Side	Average depth (mm)	Average speed (m/s)
90	0	2.995	-0.963	0.042	98	0.38
	5	3.071	-0.835	0.016	102	0.38
	15	3.371	-0.658	0.026	112	0.36
	20	2.724	-0.079	0.053	110.33	0.36
	30	2.212	-0.057	0.005	102.66	0.38
25	0	0.309	-0.172	-0.879	36.33	0.39
	5	1.896	-0.238	-1.112	109.00	0.36
	15	2.152	-0.102	11.123	117.33	0.34
	20	1.677	0.062	-0.778	115.33	0.34
	30	1.535	0.009	-0.619	105.33	0.37

N.B. See Figure B.1.

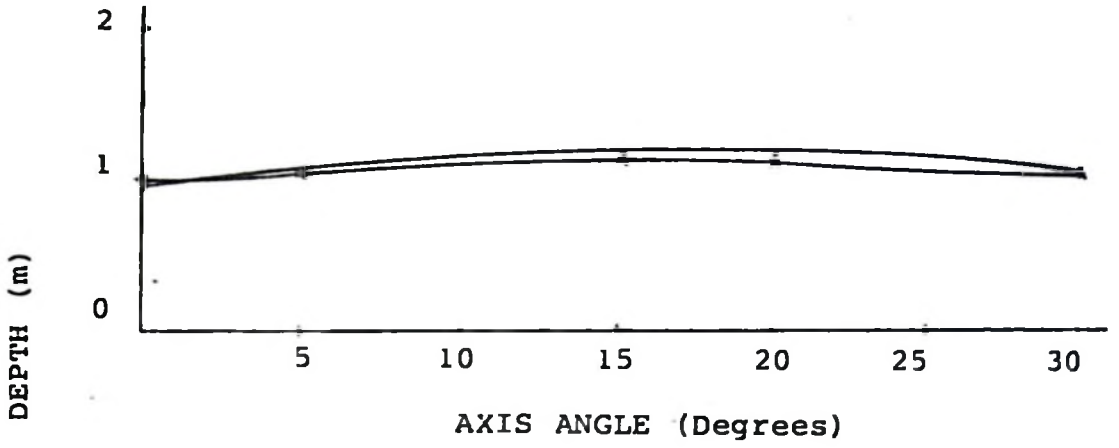

Figure B.1(a) Effect of axis angle on depth

x = 90° sweep angle
. = 25° sweep angle

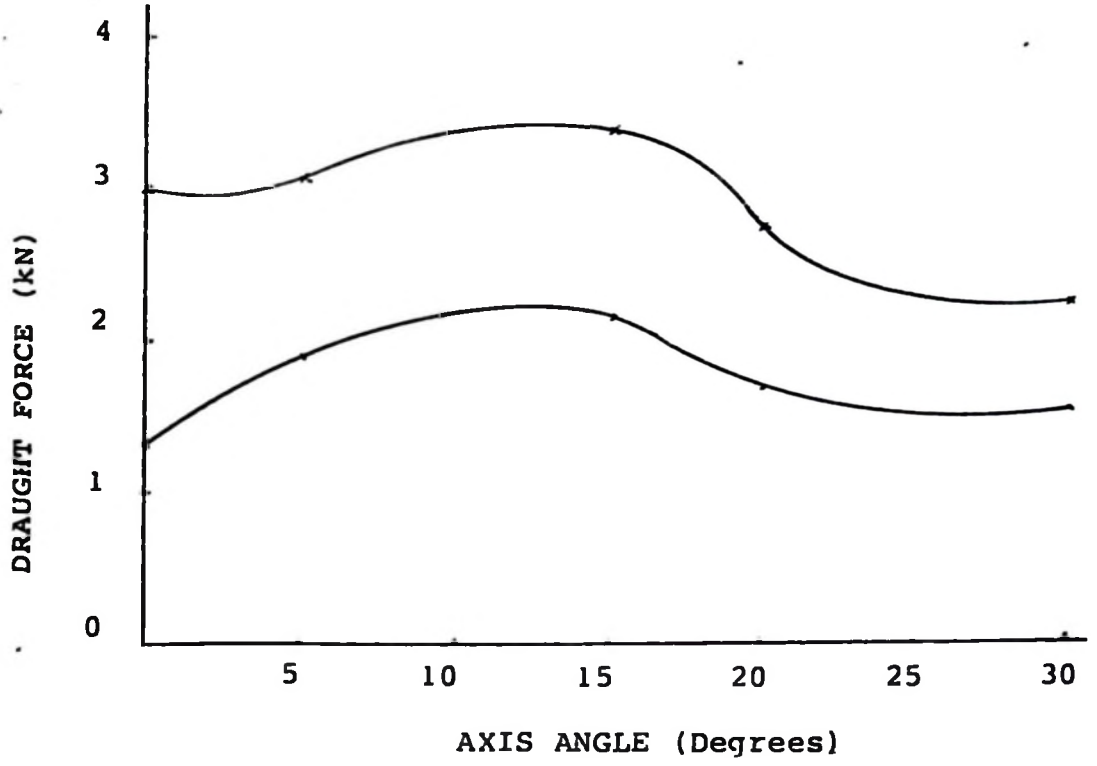

Figure B.1(b) Effect of axis angle on draught

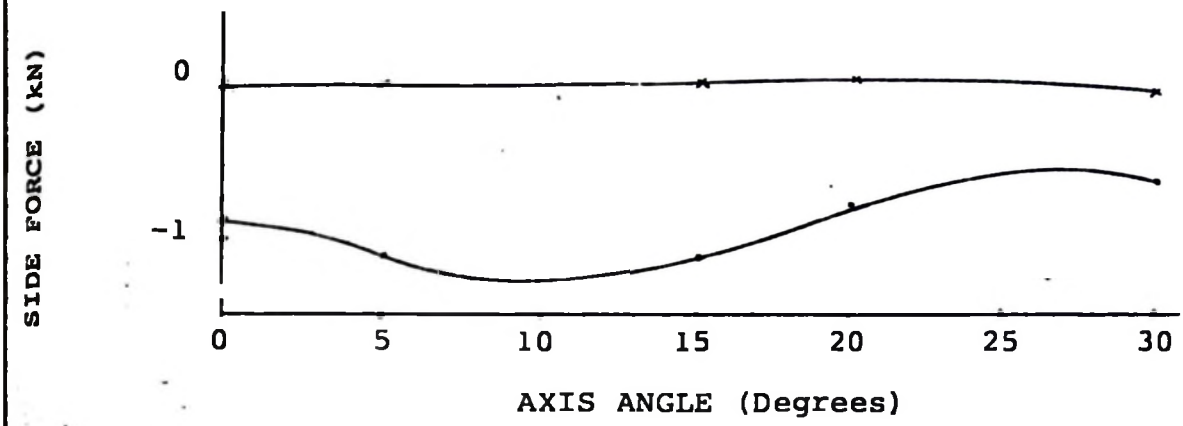

Figure B.1(c) Effect of axis angle on side force

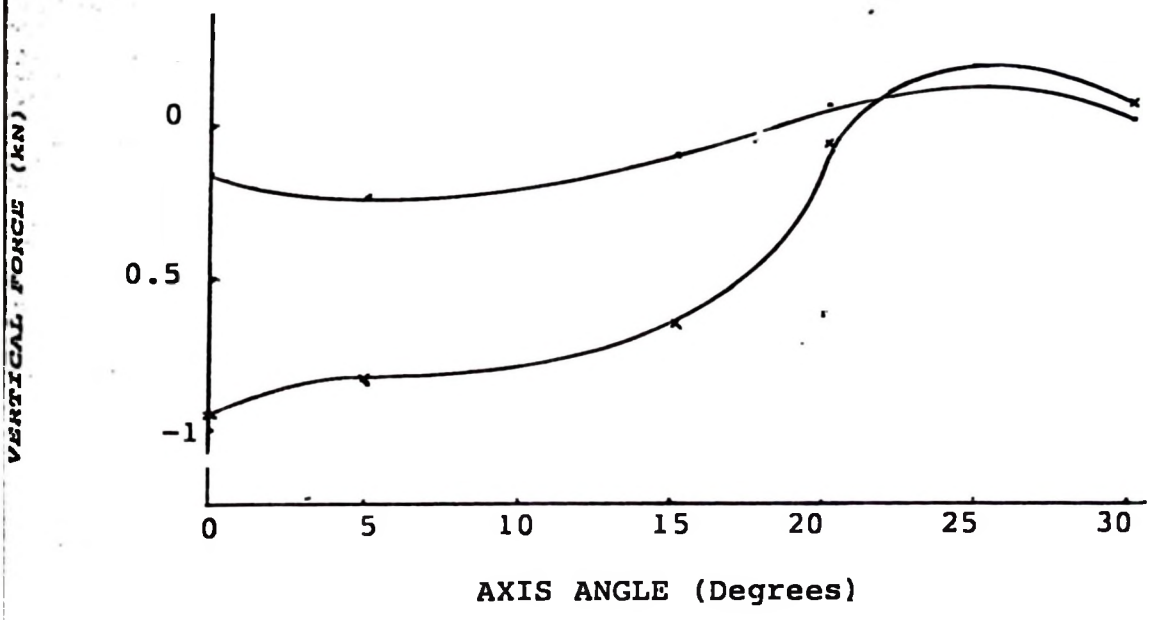

Figure B.1(d) Effect of axis angle on vertical force

APPENDIX C : SUMMARY OF MOISTURE CONTENT AND BULK DENSITY CALCULATIONS

(i) Calculation of moisture content (dry base):

$$\frac{\text{Weight of wet soil - Weight of dry soil}}{\text{Weight of dry soil}} \times 100\%$$

(ii) Calculation of bulk density:

$$\frac{\text{Weight of undisturbed soil (wet or dry)}}{\text{Volume of cylinder}}$$

(iii) Calculation of bulk unit weight :

$$\text{Bulk density (wet or dry)} \times 9.81\ kN/m^3$$

(iv) Summary for moisture content and bulk density

Batch	Moisture Content (dry base) %	Bulk density (g/cc)		Bulk unit weight (kN/m^3)	
		Wet	Dry	Wet	Dry
1	8.66	1.52	1.37	14.91	13.44
2	8.80	1.54	1.35	15.11	13.24
3	8.60	1.51	1.38	14.81	13.54
4	8.50	1.51	1.38	14.81	13.54
5	8.66	1.52	1.37	14.91	13.44
6	8.37	1.49	1.39	14.62	13.64
7	8.53	1.51	1.38	14.81	13.54
Average	8.60	1.51	1.38	14.81	13.54

APPENDIX D : PREDICTION OF DISC FORCES

Parameters

Depth of work d = 0.1

Bulk unit weights: wet γ_i = 14.81 kN/m³ dry γ_f = 13.54 kN/m³

Cohension C = 10.2 kN/m²

Angle of internal shearing resistance $\phi = 40^o$

Angle of soil metal friction $\delta = 22^o$

Adhesion Ca= 0 kN/m²

Radius of disc R = 0.305 m

Sweep angle $\theta = 90^o$ and 25^o

Passive cutting reaction = P kN

N_γ, N_{ca}, N_q are dimensionless numbers

$$P = (\gamma_i d^2 N_\gamma + cdN_{ca} + (R-d)\ \gamma_f \sin' \theta dN_q)\sqrt{2Rd-d^2}\ \text{Sin}\ \theta$$

Determination of rake angle was done using the method given by Godwin et al (8) and the results obtained as below:

Axis angle (^{o})	Rake angle (α) (^{o})
0	65
5	60
15	50
20	45
30	35

Calculation of concave (facial) force

Determination of N factors

$\alpha = 65^o$ $\phi = 40^o$

$N_{\gamma\delta} = 0 = 1.25$

$N_{\gamma\delta} = \phi = 4.3$

Hence $N_{\gamma\delta = 22^o} = 1.25 \left(\frac{4.3}{1.25}\right)^{\frac{22}{40}} = 2.47$

$N_{c\delta} = 0 = 1.7$

$N_c A_\delta = \phi = 8.2$

$Ca = c$

Hence $N_{ca\delta} = 22^o = 1.8 \left(\frac{8.2}{1.8}\right) \frac{22}{40} = 4.14$

$N_{q\delta} = 0 = 2.5$

$N_{q\delta} = \phi = 7.5$

Hence $N_{q\delta} = 22^o = 2.5 \left(\frac{7.5}{2.5}\right) \frac{22}{40} = 4.57$

$$P = \{(14.81\ kN/m^3 \times 0.1^2 m^2 \times 2.47) + (10.2 kN/m^2 \times 0.1m \times 4.14) + (0.305 - 0.1) 13.54\ kN/m^3 \times \sin' 90^o \times 0.1m \times 4.57\} \{2 \sqrt{2 \times 0.305 \times 0.1^2} \sin 90^o\}$$

$$= \{0.365 + 4.22 + 1.268\} \{0.45166 \sin 90^o\}$$

$$= 2.644\ kN$$

For $\theta^o = 25^o$ $P = 0.978$ kN

$Hp = P \sin(\alpha + \delta) = 2.644 \sin(65^0 + 22^o) = 2.644$ kN

For $\theta = 25^o$ $Hp = 0.977$

$Vp = 1\ P \cos(\ +\ ) = -2.644 \cos 87^o = -0.138$ kN

For $\theta = 25^o$ $Vp = -0.051$ kN

$DP = Hp \sin \theta = 2.644 \sin 90^o = 2.644$ kN

For $\theta = 25^o$ $Dp = 0.413$ kN

$Sp = Hp \cos \theta = 2.644 \cos 90^o = 0$

For $\theta = 25^o$ $Sp = 0.885$ kN

<u>Calculation of convex (rear scrubbing forces)</u>

For deep spherical disc at 0.1 $\lambda = 45^o$ (λ = clearance angle)

Projected area $A = \frac{w}{2} \times \frac{x}{2}$ (where w is disc diameter and x is the depth of concavity)

For deep spherical disc at 0.1 m depth x = 0.43 m

A = 0.00656 m²

$\beta = 90 - \alpha$; so when $\alpha = 65^{o}$ $\beta = 25^{o}$

$q = cN_c$

$N_{c\delta = 0}$ for $\beta = 25^{o} = 9$

$N_{c\ \delta = \phi}$ for $\beta = 25^{o} = 70$

Hence $N_c{}'\ \delta = 22^{o} = (70-0) \times \frac{22}{40} + 9$

$= 42.55$

$q = 10.2\ kN/m^2 \times 42.55 = 434.01\ kN/m^2$

$Vs = qA \sin \left(\frac{\lambda - \theta}{\lambda}\right) 90^{o}$

For $\theta = 90^{o}$ Vs, Ds and Ss = 0

For $\theta = 25^{o}$ $Vs = 434.01\ kN/m^2 \times 00656\ m^2 \sin \left(\frac{45^{o} - 25^{o}}{45^{o}}\right) 90^{o}$

$= 1.8301\ kN$

$Ds = Vs \tan (\alpha - \delta) \sin (\lambda - \theta)$

$= 1.8301 \tan (65^{o} - 22^{o}) \sin (45^{o} - 25^{o}) = 0.5837\ kN$

$Ss = Vs \tan (\alpha - \delta) \cos (\lambda - \theta)$

$= 1.8301 \tan 43^{o} \cos 20^{o} = 1.6037\ kN$

<u>Total forces</u>

For $\theta = 90^{o}$

D = Dp + Ds = 2.64 + 0 = 2.64 kN

V = Vp + Vs = -0.138 + o = -0.138 kN

S = Sp - Ss = 0 - 0 = 0 kN

For $\theta = 25^{o}$

D = 0.413 + 0.5837 = 0.997 kN

V = -0.051 + 1.8310 = 1.779kN

S = 0.885 - 1.6037 = -0.779 kN

Summary of predicted forces

Sweep angle (°)	Axis angle (°)	Rake angle (°)	Force Draught	Vertical	Side
90	0	65	2.64	-0.14	0
90	5	60	2.23	-0.31	0
90	15	50	1.71	-0.56	0
90	20	45	1.49	-0.63	0
90	30	35	1.16	-0.75	0
25	0	65	1.00	1.78	-0.72
25	5	60	0.85	1.77	-0.65
25	15	50	0.61	1.75	-0.41
25	20	45	0.51	1.76	-0.31
25	30	35	0.34	1.86	-0.10

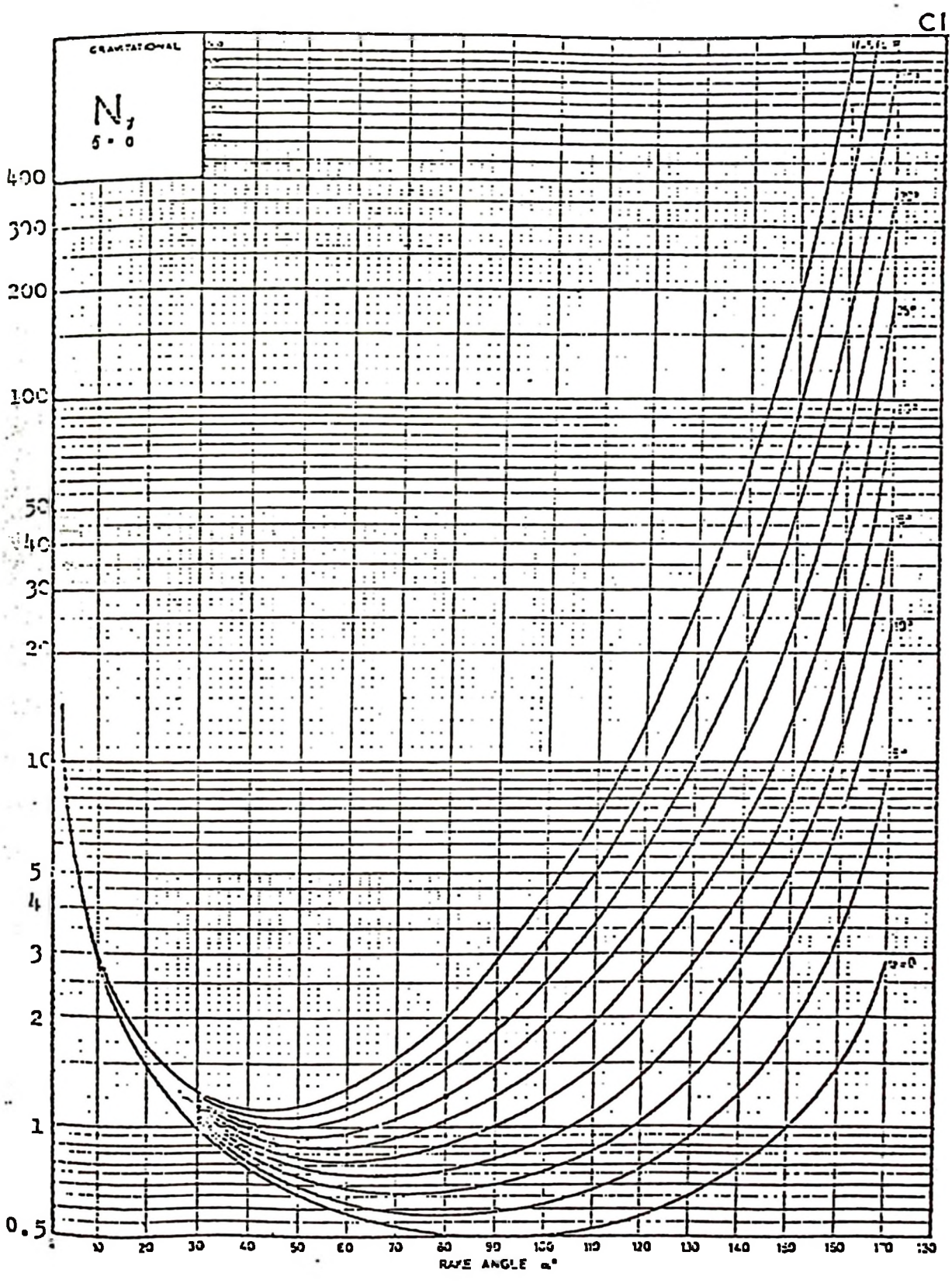
CI
GRAVITATIONAL
N_γ
5 • 0
400
300
200
100
50
40
30
20
10
5
4
3
2
1
0.5
10
20
30
40
50
60
70
80
90
100
110
120
130
140
150
160
170
180
RAKE ANGLE α°

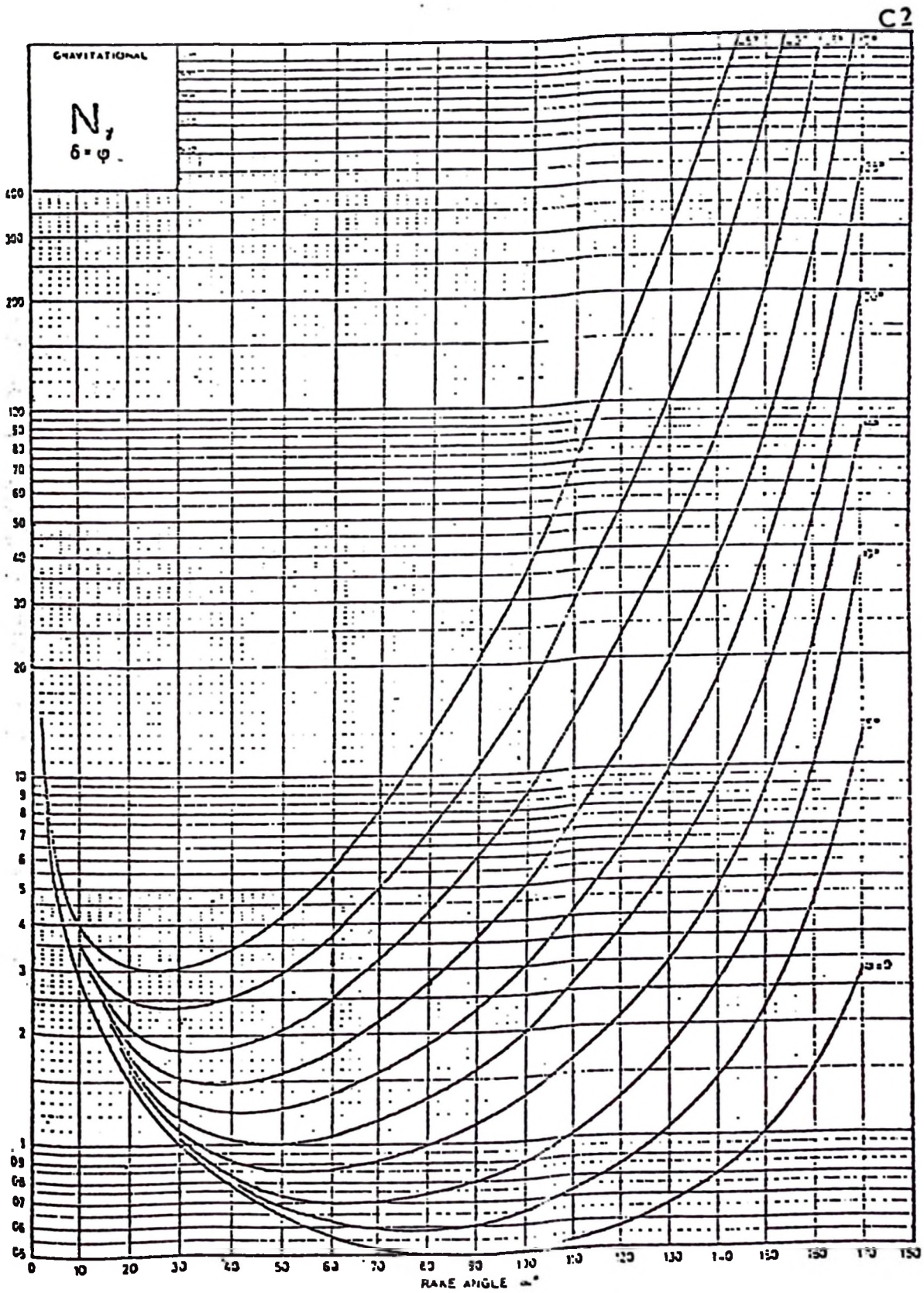
C2
GRAVITATIONAL
N_γ
$\delta = \varphi$
RAKE ANGLE

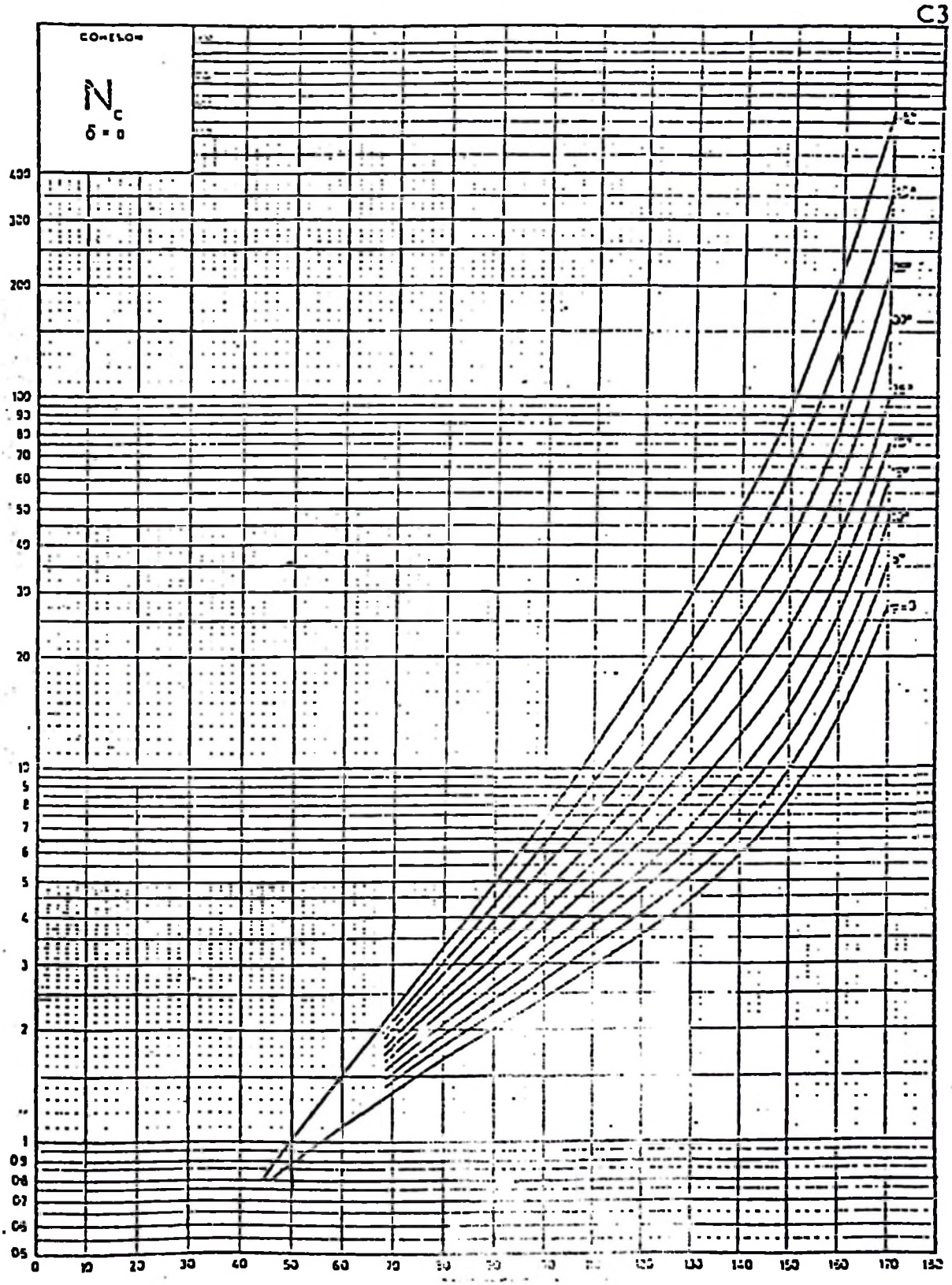
C3
CONELON
N_c
δ = 0

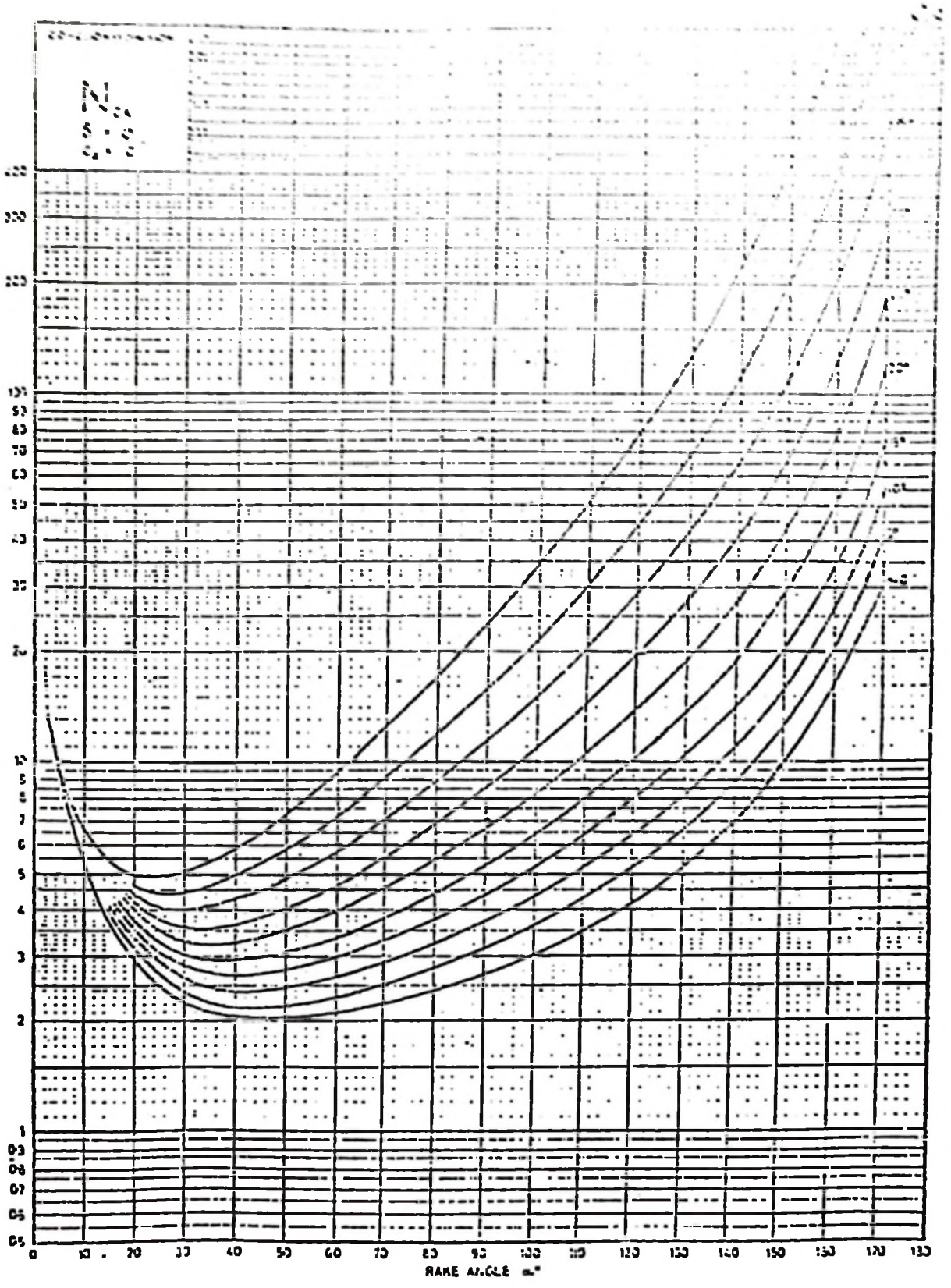
RAKE ANGLE

C5

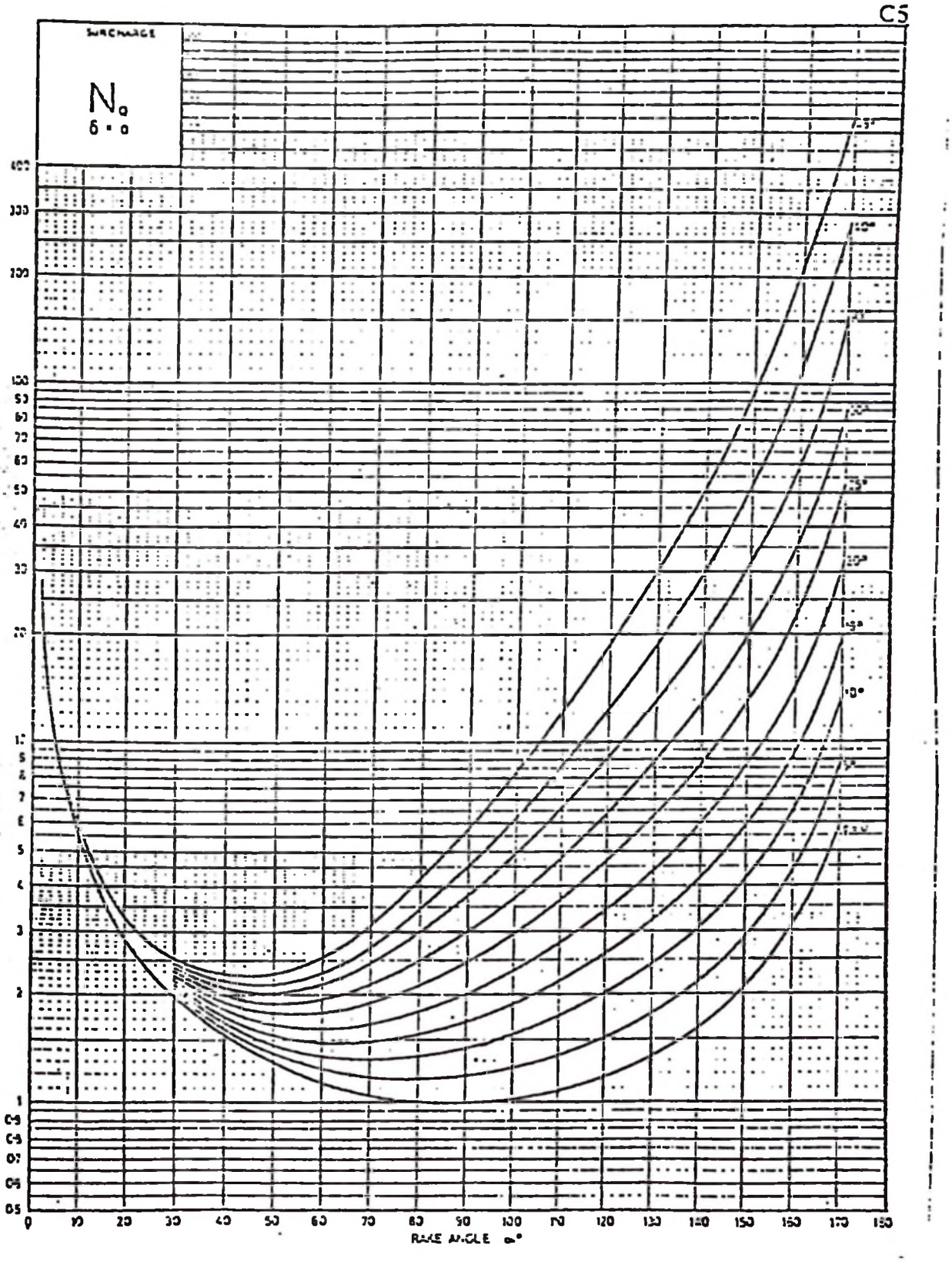

C6

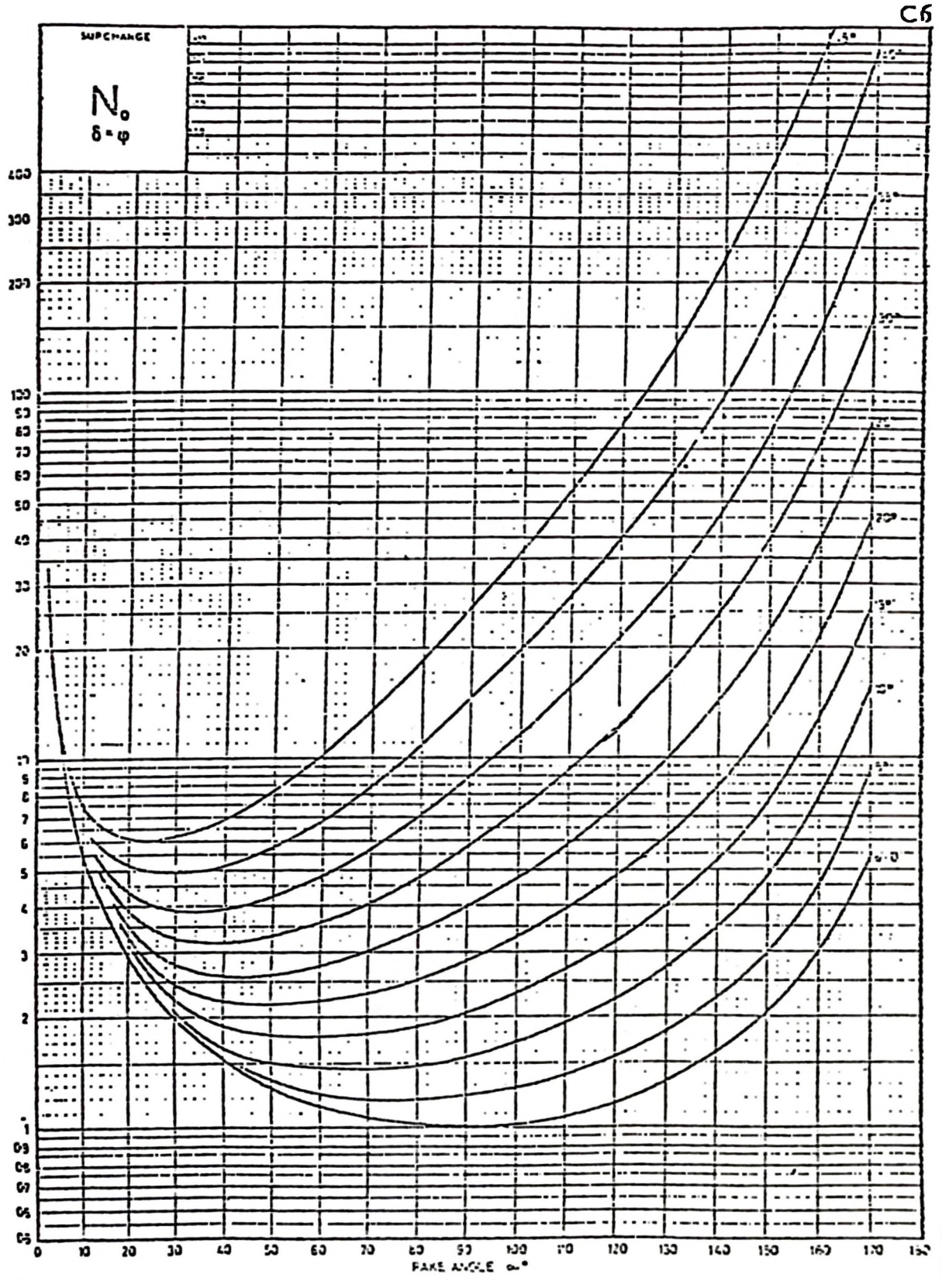
SUPCHARGE
N_o
$\delta = \varphi$
400
300
200
100
90
80
70
60
50
40
30
20
10
9
8
7
6
5
4
3
2
1
0.9
0.8
0.7
0.6
0.5
0
10
20
30
40
50
60
70
80
90
100
110
120
130
140
150
160
170
180
RAKE ANGLE α°

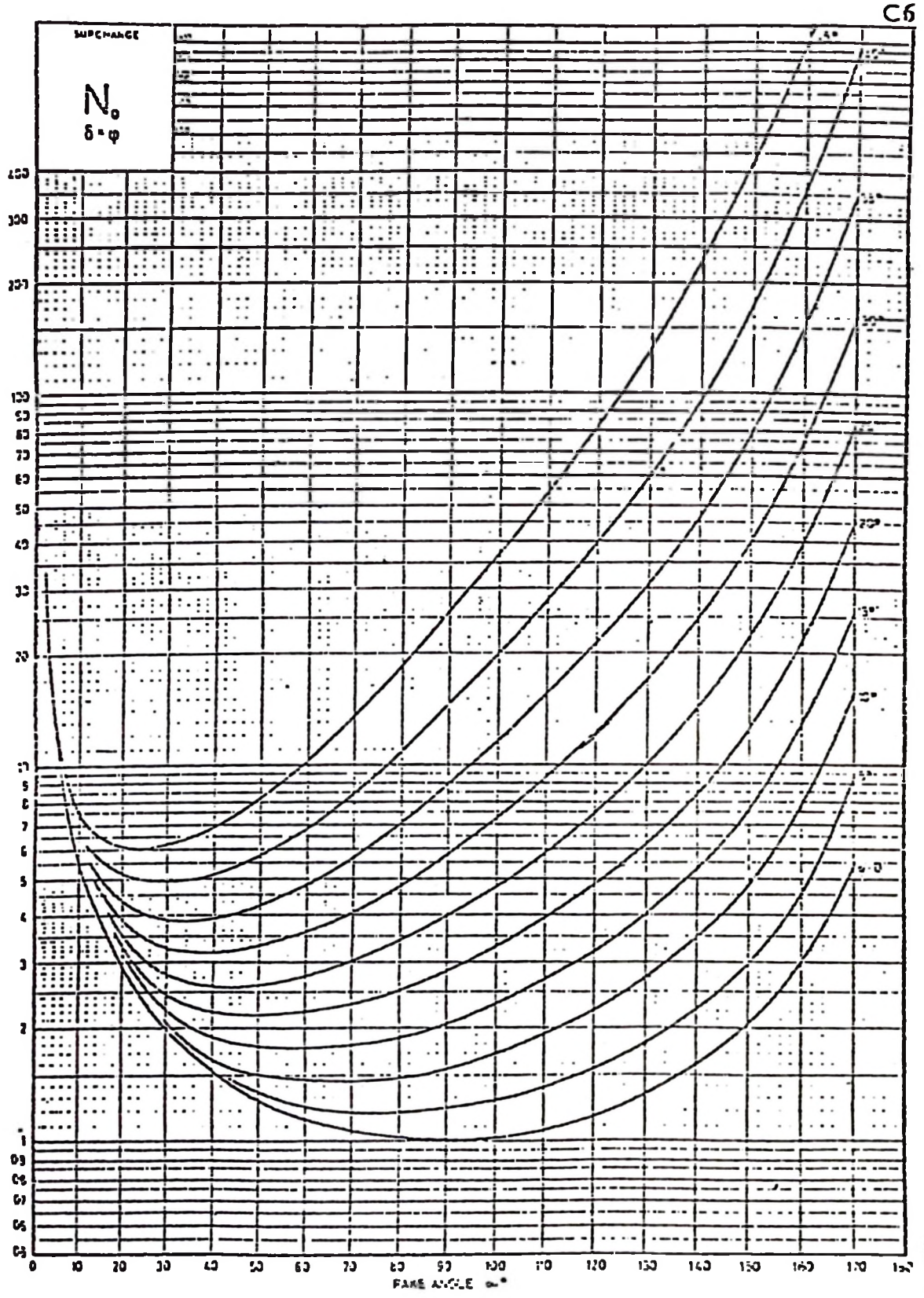
Cδ
SUPCHARGE
N_o
δ=φ
FAKE ANGLE

Bearing Capacity Factors for Wedge Footings

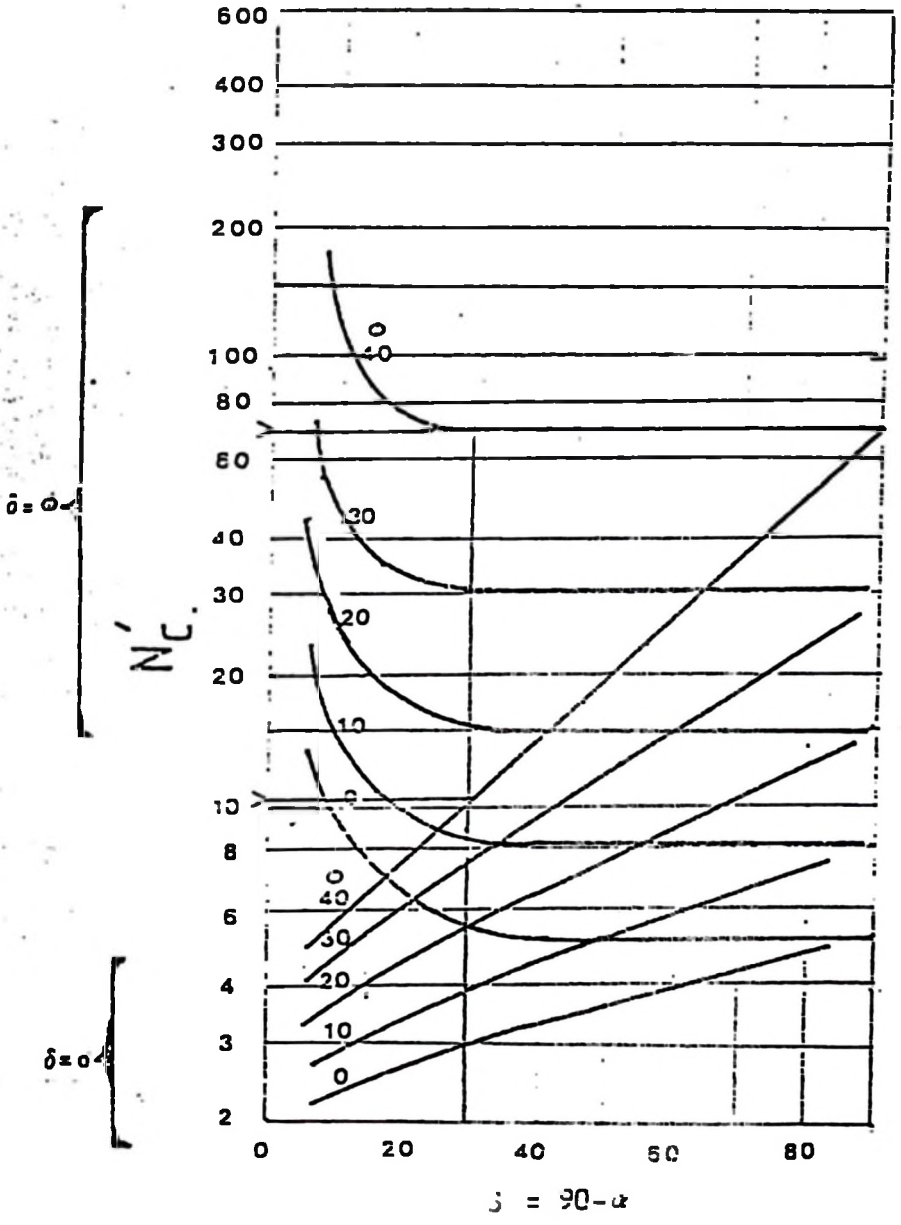

APPENDIX E : SUMMARY OF EXPERIMENTAL RESULTS

Sweep angle	Axis angle	Rake angle	Depth mm	Speed m/s	Draft force (kN)	Vertical force (kN)	Side Force (kN)
90°	0°	65°	100	0.3	2.138	0.391	0.005
	5°	60°	100	0.3	2.212	0.285	0.011
	15°	50°	100	0.3	2.145	0.079	0.032
	20°	45°	100	0.3	1.971	-0.101	0.016
	30°	35°	100	0.3	1.652	-0.206	0.026
25°	0°	65°	100	0.3	0.978	0.009	-0.568
	5°	60°	100	0.3	0.959	-0.026	-0.593
	15°	50°	100	0.3	0.918	-0.114	-0.263
	20°	45°	100	0.3	1.155	0.014	-0.393
	30°	35°	100	0.3	1.233	0.179	-0.276

APPENDIX F : STATISTICAL ANALYSIS OF EXPERIMENTAL RESULTS

The method used was the Randomized Complete-Block Design (16)

(i) Draught force with 90^{o} sweep angle:

Treatment (Axis angle) (^{o})	Block 1	2	3	4	5	6	Treatment Totals $X_{i.}$	$\Sigma_i X^2_{ij}$
0	2.235	2.235	1.967	1.877	2.301	2.2125	12.8275	27.5724
5	2.281	2.190	1.967	1.877	2.5665	2.3895	13.271	29.6879
15	2.212	2.028	2.438	2.167	2.056	1.967	12.868	27.7417
20	1.716	1.806	2.3898	2.301	1.806	1.806	11.8248	23.7353
30	1.698	1.698	1.6815	1.593	1.665	1.577	9.9125	16.3906
Block Totals) $X_{.j}$	10.142	9.957	10.4433	9.815	10.493	9.952	60.7038	
Block Totals) $\Sigma_i X^2_{ij}$	20.919	20.0489	22.2206	19.5744	22.1425	20.2225		125.1279

$X_{i.}^2 = 12.8275^2 + ... + 9.9125^2 = 744.3332$

C = Correction factor = $\frac{X_{i.}^2}{rt}$ where r = replications (blocks) = 6

t = treatments (axis angle) = 5

$= \frac{60.7038^2}{6 \times 5} = 122.8317$

Total Sum of Squares $(SS_T) = \Sigma_{ij} X^2_{ij} - C = 27.5724 + ... + 16.3906 - 122.8317$

$= 2.2962$

APPENDIX F (continued)

$$\text{Block Sum of Squares} = \frac{\sum_j X_j^2}{t} - C$$

$$= 10.142^2 + ... + 9.952^2 - 122.8317$$

$$= 0.4771$$

$$\text{Treatment Sum of Squares (TSS)} = \frac{\sum_i X_i^2}{r} - C$$

$$= \frac{12.8275^2 + ... + 9.9125^2}{6} - 122.8317$$

$$= 1.2238$$

$$\text{Error Sum of Squares (ESS)} = SS_T - BSS - TSS$$

$$= 2.2962 - 0.4711 - 1.2238$$

$$= 0.5953$$

APPENDIX F (continued)

Analysis of Variance (ANOVA) :

Source of variation	Degrees of freedom (df)	Sum of squares (SS)	Mean Sum of squares (MS)	F. Value
Block	5	0.4771	0.0954	3.2013*
Treatment	4	1.2238	0.3059	10.2651**
Error	20	0.5953	0.0298	
Total	29	2.2962		

$F\ F_{4,20,\ 0.05} = 2.87$
$F\ F_{4,20,\ 0.01} = 4.43$

∴ There is a significant difference between treatments at both 5% and 1% levels.

At 5% level, there is a significant difference between blocks.

Least significant difference (lsd) test:

$$lsd\ (0.05) = t._{05}sd = 2.086\ \sqrt{\frac{2 \times 0.0298}{6}} = 0.2079$$

$$lsd\ (0.01) = t._{01}sd = 2.845\ \sqrt{\frac{2 \times 0.0298}{6}} = 0.2835$$

where 2.086, 2.845 are $t_{4,20}$ values from tables at 5% and 1% levels respectively.

0.1298 = Error Mean Square from ANOVA table above.

6 = r - number of replications.

Treatments	Mean ($\bar{x}$)	Difference between means:
0^o	2.1379	0.0739
5^o	2.2118	
15^o	2.1447	0.0671
20^o	1.9708	0.1739
30^o	1.6521	0.3187

∴ There is significant difference between 20^o and 30^o axis angle

APPENDIX F (continued)

(ii) Draught force with 25^{o} sweep angle

Treatment (Axis angle) (^{o})	Block 1	2	3	4	5	6	$X_{i.}$	Treatment Totals $\Sigma_i X^2_{ij}$
0	0.993	0.903	0.993	1.084	0.993	0.903	5.869	5.764
5	1.084	0.993	0.821	0.821	1.062	0.9735	5.7545	5.5847
15	0.983	1.073	0.9735	0.7965	0.7965	0.885	5.5075	5.1174
20	1.073	1.162	1.0837	1.2643	1.174	1.174	6.931	8.0310
30	1.162	1.162	1.341	1.341	1.239	1.1505	7.3955	9.1558
Block Totals $X_{.j}$	5.2950	5.2930	5.2122	5.3068	5.2645	5.0860	31.4575	
Block Totals $\Sigma_i X^2_{ij}$	5.629	5.6533	5.5805	5.8802	5.6617	5.2483		33.653

$X_{i.}^2$ = 200.6242 SS_T = 0.6672 TSS = 0.4516

C = 32.9858 BSS = 0.0071 ESS = 0.2085

APPENDIX F (continued)

ANOVA

Source of variation	df	SS	MS	F
Blocks	5	0.0071	0.0014	0.1346 NS
Treatments	4	0.4516	0.1129	10.8558 **
Error	20	0.2085	0.0104	
Total	29	0.06672		

$F > F_{4, 20, 0.05} = 2.87$ } Significant difference existed between
$F > F_{4, 20, 0.01} = 4.43$) treatments at 5% and 1% levels

LSD Test:

lsd (0.05) = t 0.05 sd = 0.1228
lsd (0.01)=t 0.01 sd = 0.1675

Treatment	Mean ($\bar{x}$)	Difference between means
0^o	0.9782 }	0.0191
5^o	0.9591 }}	
15^o	0.9179 }}	0.0412
20^o	1.1552 }}	-0.2373
30^o	1.2326 }	-0.0774

∴ There is a significant difference between 15^o and 20^o axis angle for 5% and 1% levels.

APPENDIX F (continued)

(iii) Vertical force with 90^{o} sweep angle

Treatment (Axis angle) (^{o})	Block 1	2	3	4	5	6	Treatment totals X_i.	ΣX^2_{ij}
0	0.42	0.447	0.263	0.289	0.4776	0.4511	2.3477	0.9605
5	0.289	0.342	0.184	0.131	0.4204	0.3416	1.708	0.5449
15	0.106	0.126	0.212	0.133	0	0	0.477	0.0745
20	-0.158	-0.131	-0.0531	0	-0.131	-0.131	-0.6041	0.0793
30	-0.21	-0.184	-0.184	-0.158	-0.263	-0.263	-1.235	0.2616
Block Totals) X_j	0.447	0.5	0.4219	0.395	0.504	0.4257	2.6936	
ΣX^2_{ij}	0.3402	0.3685	0.1846	0.1433	0.4912	0.393		1.9208

Xi^2 = 10.5466 SS_T = 0.679 TSS = 1.516

C = 0.2418 BSS = 0.002 ESS = 0.161

APPENDIX F (continued)

ANOVA

Source of Variation	df	SS	MS	F
Blocks	5	0.002	0.004	0.05 NS
Treatments	4	1.514	0.379	47.375 **
Error	20	0.161	0.008	
Total	29	1.679		

$F > F_{4,20}$, 0.05 = 2.87)
$F > F$, , 0.01 = 4.43) ∴ There is significant difference between treatments at both 5% and 1% levels

LSD test:

lsd (0.05) = t 0.05 sd = 0.1077
lsd (0.01) = t 0.01 sd = 0.1469

Treatment	Mean ($\bar{x}$)	Difference between means
0	0.3913	0.1066
5	0.2847	0.2052
15	0.0795	0.1802
20	-0.1007	0.1051
30	-0.2058	

∴ There is significant difference between 5^{o} and 20^{o} axis angles at both 5% and 1% levels

(iv) Vertical force with 25^{o} sweep angle

Treatment (Axis Angle) (^{o})	Block 1	2	3	4	5	6	Treatment totals $X_{i.}$	$\sum_i X^2_{ij}$
0	0.0265	0	0	0.026	0	0	0.0525	0.0014
5	0	0	-0.026	-0.026	-0.0525	-0.0525	-0.157	0.0068
15	-0.133	-0.106	-0.0788	-0.0525	-0.158	-0.158	-0.6863	0.0878
20	0.186	0.133	-0.0788	-0.0263	-0.079	-0.0525	0.0824	0.0682
30	0.184	0.184	0.210	0.210	0.156	0.1301	1.0741	0.1972
Block Totals) X_j	0.2635	0.211	0.0264	0.1312	-0.1335	-0.1329	0.3657	
Block Totals) $\sum_i X^2_{ij}$	0.0868	0.0628	0.0572	0.0489	0.0583	0.0474		0.3614

Xi^2 = 1.6589 SS_T = 0.3569 TSS 0.272

C = 0.0045 BSS = 0.029 ESS = 0.0559

APPENDIX F (continued)

ANOVA

Source of variation	df	SS	MS	F
Blocks	5	0.029	0.0058	2.0714 NS
Treatments	4	0.279	0.0680	24.2857**
Error	20	0.0559	0.0028	
Total	29	0.3569		

$F > F_{4,20}$, 0.05 = 2.87) Therefore there is significant
$F > F_{4,20}$, 0.01 = 4.43) difference between treatments
at 5% and 1% levels

LSD test:

lsd (0.05) = t 0.05 sd =0.0637
lsd (0.01) = t o.01 sd = 0.0869

Treatment	Mean ($\bar{x}$)	Difference between means
0^o	0.00875	0.03459
5^o	-0.0262	0.0882
15^o	-0.1144	0.1281
20^o	0.0137	-0.1653
30^o	0.1790	

∴ There is significant difference between 5^o and 30^o axis angle at 5% and 1% levels

APPENDIX F (continued)

(v) Side force with 90^{o} sweep angle

Treatment (Axis angle) (^{o})	Block 1	2	3	4	5	6	Treatment total $X_i.$	$\sum_1 X^2_{ij}$
0	0	-0.032	0	0	0	0	-0.032	0.001
5	0	0	0	0	0.0321	0.0321	0.0642	0.0021
15	0.0635	0.0635	0	0.032	0	0.031	0.19	0.01
20	0.032	0.032	0	0	0.032	0	0.096	0.0031
30	0	0	0.032	0	0.0635	0.0635	0.159	0.0091
Block Totals) X_j	0.0955	0.0635	0.032	0.032	0.1276	0.1266	0.4772	
$\sum_1 X^2_{ij}$	0.0051	0.0061	0.001	0.001	0.0061	0.006		0.0253

$X_{i.}^2$ = 0.0757 SS_T = 0.0177 TSS = 0.005

C = 0.0076 BSS = 0.0019 ESS = 0.011

APPENDIX F (continued)

ANOVA

Source of variation	df	SS	MS	F
Blocks	5	0.0019	0.0004	0.8 NS
Treatments	4	0.005	0.0012	2.4
Error	20	0.011	0.0005	
Total	29	0.0177		

$F > F_{4,20,\ 0.05} = 2.87$)
) ∴ There is no significant difference between treatments at 5% and 1%
$F > F_{4,20,\ 0.01} = 4.43$)

LSD test:

lsd (0.05) = $t_{0.05} = 0.0269$; lsd (0.01) = $t_{0.01} = 0.0367$

Treatment	Mean ($\bar{x}$)	Difference between means
0^{o}	0.0053 }	
		-0.0054
5^{o}	0.0107 } }	
		-0.021
15^{o}	0.0317 } }	
		0.0157
20^{o}	0.0160 } }	
		-0.0105
30^{o}	0.0262 }	

∴ There is no significant difference between the treatments.

(vi) Side force with 25^{o} Sweep angle

Treatment (Axis angle) (^{o})	Block 1	2	3	4	5	6	Treatment total Xi.	$\sum_i X^2_{ij}$
0	-0.513	-0.449	-0.604	-0.667	-0.6035	-0.5718	-3.4083	1.9655
5	-0.609	-0.545	-0.449	-0.449	-0.7699	-0.7378	-3.5597	2.2082
15	-0.458	-0.458	-0.4765	-0.445	-0.44	-0.472	-2.7495	1.2610
20	-0.353	-0.417	-0.3812	-0.445	-0.381	-0.381	-2.3582	0.9322
30	-0.222	-0.222	-0.321	-0.353	-0.254	-0.286	-1.658	0.4725
Block (X.j	-2.155	-2½091	-2.2317	-2.359	-2.4484	-2.4484	13.7337	
Totals ($\sum_i Xij^2$	1.0177	0.9316	1.0418	1.1671	1.3602	1.3210		6.8394

Xi^2 = 40.1578 SS_T = 0.5523 TSS = 0.4059

C = 6.2871 BSS = 0.0233 ESS = 0.1231

ANOVA

Source of Variation	df	SS	MS	F
Blocks	5	0.0233	0.0047	0.7705 NS
Treatments	4	0.4059	0.1015	16.6393**
Error	20	0.1231	0.0061	
Total	29	0.5523		

$F > F_{4,20}$, 0.05 = 2.87 ∴ There is significant differen
$F > F_{4,20}$, 0.01 = 4.43 between treatments at 5% and 1% levels

LSD test:

lsd (0.05) = $t_{0.05}$sd = 0.0941

lsd (0.01) = $5_{0.01}$sd = 0.1283

Treatment	Mean ($\bar{x}$)	Difference between means
0^o	-0.56805}	0.02525
5^o	-0.5933 }}	-0.1353
15^o	-0.458 }}	-0.065
20^o	-0.393 }}	-0.1173
30^o	-0.2757 }	

∴ At 5% levels there is a significant difference between 5^o and 15^o and 20^o and 30^o.
At 1% levels there is a significant difference between 5^o and 15^o